

## Luminescent Rhenium and Ruthenium Complexes of an Amphoteric Poly(amidoamine) Functionalized with 1,10-Phenanthroline

Daniela Maggioni,<sup>\*,†</sup> Fabio Fenili,<sup>†</sup> Laura D'Alfonso,<sup>‡</sup> Daniela Donghi,<sup>†,⊥</sup> Monica Panigati,<sup>†,∇</sup> Ivan Zanoni,<sup>§</sup> Roberta Marzi,<sup>§</sup> Amedea Manfredi,<sup>†</sup> Paolo Ferruti,<sup>†,∇</sup> Giuseppe D'Alfonso,<sup>†,∇</sup> and Elisabetta Ranucci<sup>\*,†</sup>

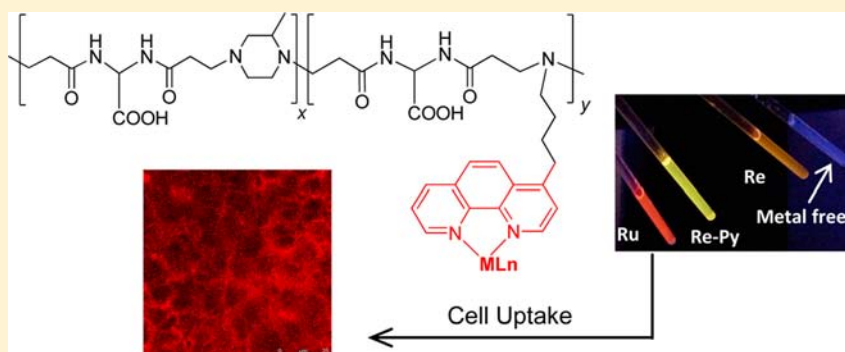
<sup>†</sup>Dipartimento di Chimica, Università degli Studi di Milano, Via Golgi 19, 20133 Milano, Italy

<sup>‡</sup>Dipartimento di Fisica, Università di Milano Bicocca, Piazza della Scienza 3, 20126 Milano, Italy

<sup>§</sup>Dipartimento di Biotecnologie e Bioscienze, Università di Milano-Bicocca, Piazza della Scienza 2, 20126 Milano, Italy

<sup>∇</sup>Consorzio Interuniversitario Nazionale per la Scienza e Tecnologia dei Materiali (INSTM), via G. Giusti 9, 50121 Firenze, Italy

**S** Supporting Information



**ABSTRACT:** A new amphoteric copolymer, **PhenISA**, has been obtained by copolymerization of 4-(4'-aminobutyl)-1,10-phenanthroline (BAP) with 2-methylpiperazine and bis(acrylamido)acetic acid (BAC) (6% of phenanthroline-containing repeating units). The copolymer showed excellent solubility in water, where it self-aggregated to give clear nanoparticle suspensions (hydrodynamic diameter =  $21 \pm 2$  nm, by dynamic light scattering (DLS) analysis). The phenanthroline pendants of the polymer stably coordinated either  $\text{Re}(\text{CO})_3^+$  or  $\text{Ru}(\text{phen})_2^{2+}$  fragments, affording luminescent **Re-PhenISA**, **Re-Py-PhenISA**, and **Ru-PhenISA** polymer complexes, emitting from triplet metal-to-ligand charge transfer ( $^3\text{MLCT}$ ) excited states (with  $\lambda_{\text{em}} = 608, 571,$  and  $614$  nm, respectively, and photoluminescence quantum yields  $\Phi_{\text{em}} = 0.7\%, 4.8\%,$  and  $4.1\%$ , in aerated water solution, respectively). DLS analyses indicated that the polymer complexes maintained the nanosize of **PhenISA**. All the complexes were stable under physiological conditions (pH 7.4, 0.15 M NaCl) in the presence of an excess of the ubiquitous competitor cysteine. In vitro viability assays showed no toxicity of **Re-Py-PhenISA** and **Ru-PhenISA** complexes, at concentrations in the range of  $0.5\text{--}50 \mu\text{M}$  (calculated on the metal-containing unit), toward HEK-293 (human embryonic kidney) cells. A preliminary investigation of internalization in HEK-293 cells, by means of fluorescence confocal microscopy, showed that **Ru-PhenISA** enters cells via an endocytic pathway and, subsequently, homogeneously diffuse within the cytoplasm across the vesicle membranes.

## INTRODUCTION

Metal coordination chemistry, in recent years, has provided a significant contribution to the development of efficient diagnostic and therapeutic agents for biomedical applications.<sup>1</sup> For instance, the use of lanthanide complexes for magnetic resonance imaging is well-established,<sup>2</sup> and many metal radionuclides, strongly chelated by suitable ligands, are extensively employed for radio-imaging and radiotherapy.<sup>3</sup> Moreover, luminescent transition-metal complexes have a definite potential for optical imaging and offer considerable advantages, with respect to organic fluorophores,<sup>1,4</sup> because of their generally high photostability,<sup>5</sup> large Stokes' shifts, and

relatively long lifetimes of the excited states. These properties permit one to overcome some drawbacks of organic fluorophores, such as photobleaching and superposition of short-lived cell autofluorescence, improving the sensitivity of the measurements.

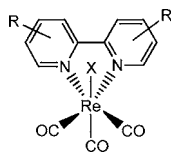
Diimine complexes of *fac*- $\text{Re}(\text{CO})_3$  are currently attracting much interest for their remarkable photophysical and photochemical properties, relevant for widespread applications in chemical and biological sensing,<sup>6</sup> bioconjugation,<sup>7</sup> and

Received: July 24, 2012

Published: November 14, 2012

optoelectronics.<sup>8</sup> Most of these studies concerned compounds with general formula  $fac\text{-}[\text{ReX}(\text{CO})_3(\text{N}^{\wedge}\text{N})]^{n+}$  (Chart 1),

**Chart 1. Schematic Drawing of the  $fac\text{-}[\text{ReX}(\text{CO})_3(\text{N}^{\wedge}\text{N})]^{n+}$  Complexes**



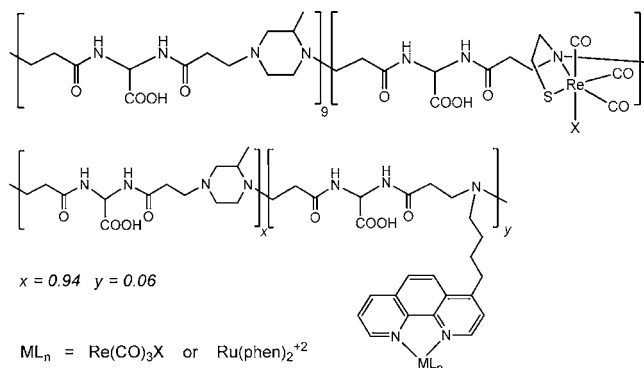
where  $\text{N}^{\wedge}\text{N}$  indicates a chelating diimine ligand (typically 2,2'-bipyridine or 1,10-phenanthroline), and X is a neutral or anionic monodentate ligand (with  $n = 1$  or 0, respectively).<sup>9,10</sup> Similar to other  $d^6$  transition-metal complexes, these species exhibit an intense long-lived emission, originating from  $d_n(\text{Re})-\pi^*(\text{N}^{\wedge}\text{N})$  triplet metal-to-ligand charge transfer ( $^3\text{MLCT}$ ) excited states. The strongest emission occurs either from mononuclear cationic complexes<sup>11</sup> or from dinuclear species in which two metal centers are bonded to the same chromophore.<sup>12–14</sup>

In this context, increasing attention is presently being focused on the covalent binding of metal complexes to water-soluble, biocompatible, and biodegradable polymer carriers,<sup>15</sup> capable of improving dispersibility in aqueous media, increasing plasma residence time, and reducing toxicity.<sup>16</sup> In addition, polymer carriers may elicit passive targeting to solid tumors via the so-called “enhanced permeability and retention” (EPR) effect,<sup>17</sup> and favor active targeting to specific tissues if decorated with suitable directing units. Moreover, the presence of numerous conjugation sites also allows one to combine different imaging functionalities on a single macromolecular carrier, for obtaining multimodal imaging probes.<sup>18</sup>

Poly(amidoamine)s (PAAs) are a family of synthetic polymers characterized by the presence of amide and *tert*-amine groups regularly arranged along the polymer chain.<sup>19</sup> They are obtained by Michael stepwise polyaddition of amines and bisacrylamides in aqueous solution and at room temperature. Under these conditions, the presence of several other functional groups does not interfere in the Michael reaction and the structure and the physicochemical properties of PAAs can be tuned within ample limits.<sup>20</sup> PAAs are normally degradable in aqueous media at  $\text{pH} > 7$ , and most of them are biocompatible, even if they are of a polycationic nature.<sup>21</sup> Some purposely planned PAAs are internalized in cells and act as endosomolytic polymers with the potential for the intracellular delivery of genes and toxins.<sup>22</sup> An amphoteric PAA carrying carboxyl groups as side substituents, namely ISA23, was determined to be almost as biocompatible as dextran and, when injected into animals, exhibited “stealth-like” properties and an EPR effect.<sup>23</sup> In a previous paper,<sup>24</sup> a tricarbonyl rhenium(I) complex of a thiol-functionalized ISA23 polymer, named ISA23SH (Chart 2), which was chosen as a model of  $^{188/186}\text{Re}$  and  $^{99\text{m}}\text{Tc}$  radiopharmaceuticals,<sup>25</sup> was reported.

Therefore, it was of interest to investigate the covalent binding of luminescent  $\text{Re}(\text{CO})_3(\text{N}^{\wedge}\text{N})^+$  moieties to a PAA backbone, to combine the excellent emission properties of the former with the good physicochemical and biological properties of the latter as carrier. In addition, the presence of many luminescent groups on the same polymeric unit could improve

**Chart 2. (Top) The Previously Reported  $\text{Re}(\text{CO})_3\text{-ISA23SH}$  Complex<sup>24</sup> and (Bottom) the  $\text{ML}_n\text{-PhenISA}$  Polymer Complexes Described Here**



the brightness of the probe itself,<sup>26</sup> since many emitters are simultaneously delivered to the same target.

Recently, dendritic ruthenium(II)-based dyes have been proposed, for diagnostic or therapeutic applications.<sup>26</sup> Dendrimers, which are a class of polymers that can be designed to have well-defined hyperbranched structures and size, may no doubt constitute an effective starting platform for obtaining multifunctional conjugates of therapeutic or diagnostic interest. Linear PAAs can be employed for the same purposes, with the additional advantage of their simple one-pot preparation process, performed in water with no added catalysts.

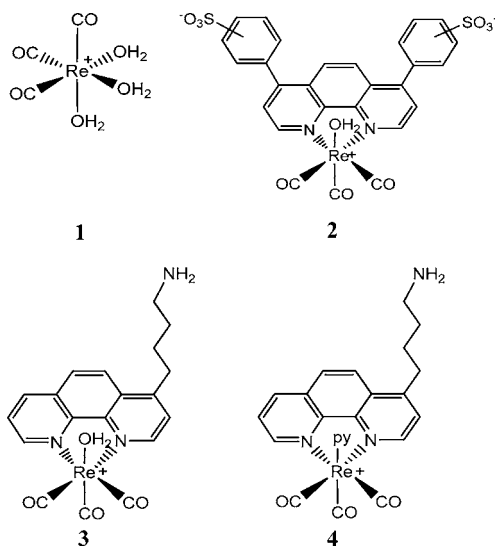
This paper describes the design and the synthesis of a new amphoteric PAA copolymer carrying a limited, but controlled, number of 1,10-phenanthroline (phen) pendants randomly distributed along the polymer chain. In aqueous media, these substituents induce spontaneous self-assembling of the PAA copolymer into nanoparticles, most likely due to hydrophobic interactions. However, it may be observed that linear PAAs, including the one employed in this work as a carrier, as a rule, enter cells and undergo intracellular trafficking, even in the absence of hydrophobic side substituents.<sup>19</sup>

The new copolymer, dubbed **PhenISA** because its major component is the constituent of the aforementioned homopolymer ISA23, was observed to be capable of tightly binding both  $\text{Re}(\text{CO})_3^+$  and  $\text{Ru}(\text{phen})_2^{2+}$  fragments (Chart 2), giving stable, water-soluble, biocompatible and highly luminescent complexes. Metal complexes of polymers containing bipyridine or phenanthroline ligands have been reported in the literature, mainly for optoelectronic applications;<sup>27</sup> however, to the best of our knowledge, this is the first time in which highly water-soluble metal complexes of a diimine-functionalized hydrophilic linear polymer are reported and proposed for imaging application.<sup>28–31</sup>

## RESULTS AND DISCUSSION

The aim of this work was to obtain a new luminescent  $\text{Re}(\text{CO})_3(\text{N}^{\wedge}\text{N})^+\text{-PAA}$  complex with the potential for imaging application. Two different strategies were devised to achieve this. The first strategy relied on the well-known affinity of metals in low oxidation states for soft sulfur ligands and consisted of preparing a complex between a luminescent  $\text{Re}(\text{CO})_3(\text{N}^{\wedge}\text{N})^+$  fragment and the previously mentioned ISA23SH copolymer (Chart 2), acting as a “multicenter” ligand through its thiol pendant groups. To this purpose, the  $[\text{Re}(\text{CO})_3(\text{OH}_2)(\text{BPS})]^-$  complex (**2** in Chart 3),<sup>32</sup> containing the water-soluble dianionic bathophenanthroline sulfonate

**Chart 3. Structures of the Complexes**  $[\text{Re}(\text{CO})_3(\text{OH}_2)_3]^+$  (1),  $[\text{Re}(\text{CO})_3(\text{OH}_2)(\text{BPS})]^-$  (2),<sup>a</sup>  $[\text{Re}(\text{CO})_3(\text{OH}_2)(\text{BAP})]^+$  (3),<sup>b</sup> and  $[\text{Re}(\text{CO})_3(\text{py})(\text{BAP})]^+$  (4)



<sup>a</sup>BPS = bathophenanthroline sulfonate, with sulfonate groups in meta or para positions. <sup>b</sup>BAP = 4-(4'-aminobutyl)-1,10-phenanthroline).

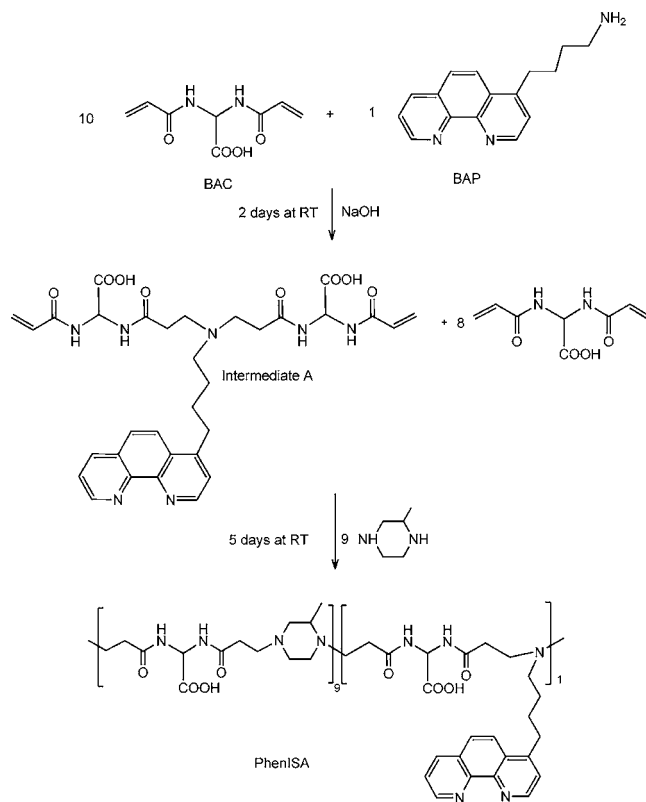
chromophore (BPS), was synthesized, via the reaction of BPS with an equimolar amount of the  $[\text{Re}(\text{CO})_3(\text{OH}_2)_3]^+$  complex (1 in Chart 3). The reaction of 2 with ISA23SH (1:1 2/SH molar ratio, 80 °C, 5 h under inert atmosphere) resulted in the replacement of the labile water ligand by the ISA23 thiol groups. The final ISA23SH- $[\text{Re}(\text{CO})_3(\text{BPS})]^-$  polymeric complex displayed the expected luminescent properties ( $\lambda_{\text{em}} = 629 \text{ nm}$ , photoluminescence quantum yields  $\Phi_{\text{em}} = 0.4\%$ ). However, incubation with an excess of the ubiquitous competitor cysteine (20 equiv) at room temperature in saline solution at pH 7.4 revealed extensive cleavage of the Re polymer bond after 24 h, pointing to the conclusion that this complex would not be endowed with long-term stability in the physiological environment. This instability is due to the fact that the polymer can bind the complex through monodentate Re–S bonds only, without the stabilization that arises from chelating N–S interactions.<sup>24</sup>

Therefore, a different strategy was envisaged, consisting of the covalent binding of the phenanthroline ligand to the polymer backbone via the insertion of limited amounts (<10%) of phenanthroline-substituted repeating units into the ISA23 chain, to obtain a copolymer capable of acting as a “multicenter” chelating ligand toward a variety of metal fragments (Chart 2).

**Synthesis of PhenISA Copolymer.** The copolymer was synthesized by the copolymerization of 4-(4'-aminobutyl)-1,10-phenanthroline (BAP), via its primary amine, with 2-methylpiperazine and bis(acrylamido)acetic acid (BAC) in 0.1:0.9:1 molar ratio (see Scheme 1). BAP was, in turn, synthesized by a slightly modified literature method (see the Experimental Section).<sup>33</sup>

In order to ensure the insertion of BAP deriving units in the final polymer chain and to randomize their distribution along the polymer chain, BAP was first reacted with 10 equiv of BAC for 48 h at room temperature, adjusting the pH to 9–10 to promote the reactivity of the terminal primary amine of BAP

**Scheme 1. Synthesis of the PhenISA Copolymer**



(Scheme 1). 2-Methylpiperazine was then added, and the reaction was allowed to proceed for 5 days at room temperature, until the final mixture became very viscous and its slightly yellow color deepened. The polymer was then isolated by acidification (pH 3) with triflic acid ( $\text{CF}_3\text{SO}_3\text{H}$ ) and ultrafiltration through a membrane with molecular weight cutoff of 3000 Da. Triflic acid was preferred to other acids in order to avoid the presence of potentially coordinating anions. Size exclusion chromatography–low angle laser light scattering (SEC-LALLS) revealed that the resultant polymer had a number-average molecular weight of  $M_n = 46\,800$  and a weight-average molecular weight of  $M_w = 83\,100$  (polydispersity index  $\text{PD} = 1.78$ ). Nuclear magnetic resonance (NMR) analysis (see below) showed that the polymer contained 94% 2-methylpiperazine deriving units and 6% phenanthroline deriving units. It may be observed that the amount of BAP units in the polymer is significantly lower than expected. This is probably due to the poor reactivity of the second hydrogen of the primary amine, which could not be completely overcome by the preliminary reaction with excess BAC.

Dynamic light scattering (DLS) measurements, performed in 0.3 M NaCl solution at pH 7.4, showed a hydrodynamic diameter of  $21 \pm 2 \text{ nm}$ , corresponding to a translational diffusion coefficient ( $D_t$ ) of  $23.8 (\pm 2.5) \mu\text{m}^2/\text{s}$ , indicating that the polymer self-assembles in aqueous media, yielding a clear nanoparticle (NP) suspension. A smaller size ( $7.6 \pm 1 \text{ nm}$ ) was measured in a different medium, which mimics the eluent used for SEC analysis (tris(hydroxymethyl)aminomethane (Tris) buffer, 0.1 M + NaCl 0.2 M). On the other hand, the SEC traces, obtained using both refractive index (RI) and light scattering (LS), gave no evidence of aggregation phenomena, suggesting that nanoaggregation is driven by reversible interactions among the macromolecular chains, easily broken

under the conditions of the SEC analysis. However, this hypothesis was not specifically investigated.

**Spectroscopic Characterization of PhenISA.**  $^1\text{H}$  diffusion ordered spectroscopy (DOSY) NMR experiments showed the same diffusion coefficient for all the resonances, both of the phenanthroline moiety and of the aliphatic backbone (Figure 1). This not only indicated that small

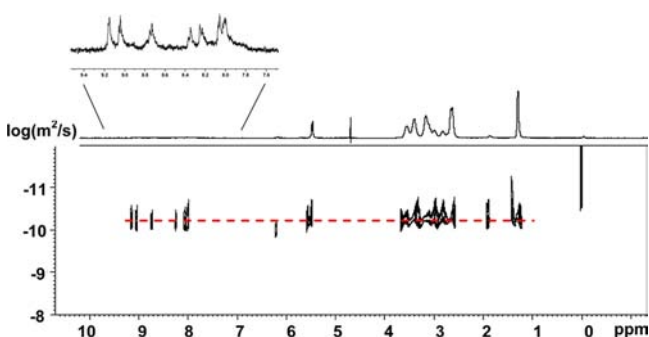


**Figure 1.** Two-dimensional (2D) map of a  $^1\text{H}$  DOSY NMR ( $\text{D}_2\text{O}$ , 300 K, 9.4 T) of PhenISA (see Experimental Section for details).

oligomers had been successfully removed, but also provided evidence of the incorporation of phenanthroline units into the macromolecular chain. Actually, the hypothesis that equidiffusion might arise from encapsulation of BAP in the polymer by hydrophobic effects was ruled out by the observation of very different diffusion coefficients for phenanthroline and ISA23 homopolymer in a DOSY experiment performed on a mixture of these two species (see Figure S1 in the Supporting Information).

A detailed multinuclear NMR characterization (including  $^{13}\text{C}$  and  $^{15}\text{N}$  NMR) was also performed. The  $^1\text{H}$  spectrum is shown in Figure 2. Concerted homonuclear and heteronuclear 2D NMR correlation spectroscopy allowed the assignment of all of the proton signals, as well as the  $^{13}\text{C}$  and  $^{15}\text{N}$  resonances (see Table S1 in the Supporting Information).

The UV spectrum of PhenISA (black trace of Figure 3a), in a pH 5.5 aqueous solution, shows a strong absorption band at ca. 200 nm, attributed to the backbone amide groups. This band and the  $\pi-\pi^*$  transitions of the phenanthroline BAP (Figure 3b)<sup>34</sup> partly overlap, so that only the BAP absorption at longer wavelength (277 nm) is detectable in the spectrum of the polymer PhenISA.

The photoluminescence (PL) spectrum of PhenISA shows a broad featureless band centered at 413 nm (Figure 3a), slightly red-shifted and broadened, with respect to the emission of the “free” (i.e., not polymer-bound) BAP ligand. The latter displays a structured band, as typical of conjugated organic molecules, with maxima at 365 and 383 nm, and approximately equispaced shoulders at higher and lower wavelength (by ca.  $1290\text{ cm}^{-1}$ ; see the gray trace of Figure 3b). The quantum yields ( $\Phi_{\text{em}}$ ) of the emission from the polymer (ca. 1%) are in agreement with the values typical of phenanthroline.<sup>35</sup>

**Synthesis of the Model Complexes  $[\text{Re}(\text{CO})_3(\text{OH}_2)(\text{BAP})]^+$  (3) and  $[\text{Re}(\text{CO})_3(\text{py})(\text{BAP})]^+$  (4).** In order to determine the best conditions for the conjugation of Re to PhenISA, the reactivity of the BAP ligand with the aquo-complex  $[\text{Re}(\text{CO})_3(\text{OH}_2)_3]^+$  (1, Chart 3) was investigated. The substitution kinetics of water by bipyridine or phenanthroline ligands in complex 1 had been previously investigated in acidic aqueous solution (pH ca. 1) at room temperature.<sup>36</sup> Under these conditions, the reaction was slow, probably because of protonation of the N atoms at low pH. On the other

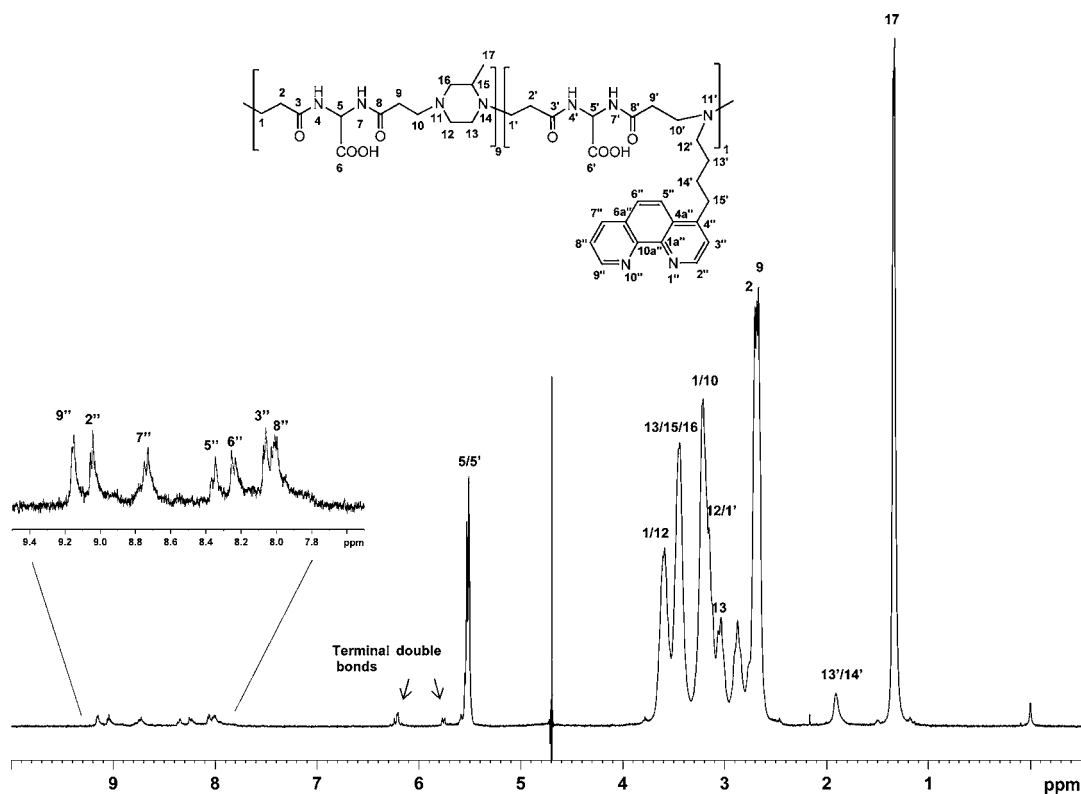


**Figure 2.**  $^1\text{H}$  NMR spectrum of PhenISA ( $\text{D}_2\text{O}$ , 300 K, 9.4 T, pH 3.2, water signal suppressed).

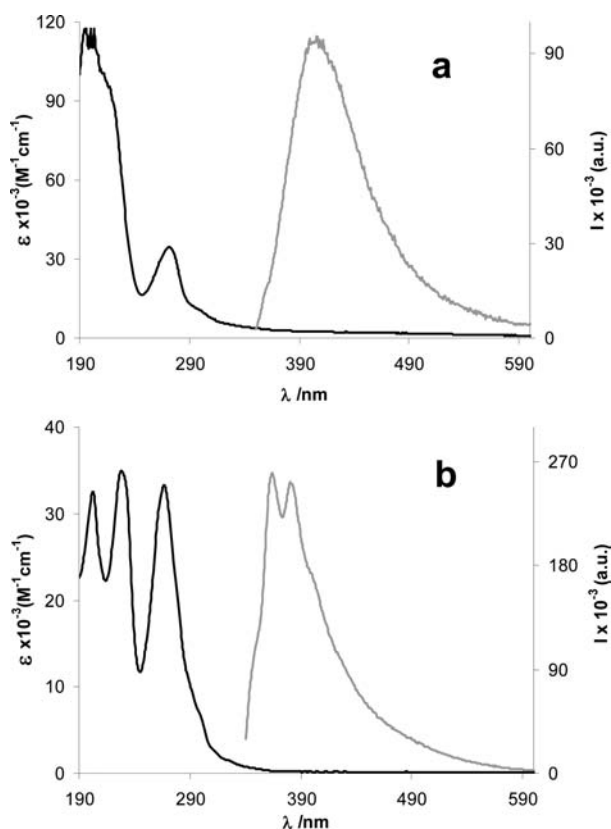


**Figure 3.** UV/vis absorption (black) and photoluminescence (gray,  $\lambda_{\text{ex}} = 320$  nm) spectra of (a) PhenISA (aqueous solution, pH 5.5) and (b) 4-(4'-aminobutyl)-1,10-phenanthroline (BAP).

hand, high pH values should be avoided, since they induce deprotonation of water ligands and condensation<sup>37</sup> to form the “cubane-like” derivative  $[\text{Re}_4(\text{CO})_{12}(\mu_3\text{-OH})_4]^{24}$ .

In the present investigation, it was found that the 1:1 reaction between  $[\text{Re}(\text{CO})_3(\text{OH}_2)_3](\text{CF}_3\text{SO}_3)$  and BAP, to give complex 3 (Chart 3), was fast when performed at pH 5.5 and at 323 K (completion occurred within 0.5 h; see Experimental Section and Figure S2 in the Supporting Information).

Phenanthroline coordination did not cause a significant change in the  $\nu(\text{CO})$  region of the IR spectrum, with respect to the spectrum of 1 (Figure S3 in the Supporting Information), in agreement with literature data for the analogous complex  $[\text{Re}(\text{CO})_3(\text{OH}_2)(\text{phen})]^+$ .<sup>38</sup> Despite its cationic nature, the emission from 3 (see Table 1) was much weaker than that of related  $[\text{Re}(\text{CO})_3(\text{L})(\text{N}^{\wedge}\text{N})]^+$  cationic complexes bearing L ligands different from  $\text{H}_2\text{O}$ . This is likely attributable to the lability of the aquo ligand and to the occurrence of hydrogen-bond and proton exchange processes (the acidity of bonded

water strongly increases in the excited MLCT state),<sup>38</sup> which can activate nonradiative deactivation pathways, resulting in a decrease in both lifetime and quantum yields. On the other hand, the intensity of the PL from 3 decreased at pH >8 (see Figure S4 in the Supporting Information), because of deprotonation of the coordinated water, to give a neutral poorly emitting hydroxo derivative.<sup>38</sup>

Therefore, to improve the emission efficiency, the synthesis of a complex containing a pyridine molecule in the sixth coordination position (complex 4 in Chart 3) was addressed, since it has already been shown that the substitution of water by pyridine in the  $[\text{Re}(\text{CO})_3(\text{OH}_2)(\text{phen})]^+$  complex affords a significant increase of the emission intensity.<sup>38</sup> Such replacement was previously performed in pyridine as solvent, and required 10 days at room temperature.<sup>38</sup> Here, reaction conditions more transferable to the polymeric ligand were found, i.e., aqueous solution, 20 equiv of pyridine, pH 5.5, 323 K for 24 h. The extent of substitution was spectroscopically determined, relying on the close analogy of the spectroscopic data of 4 (shown in Figure S5 in the Supporting Information) with the literature data for  $[\text{Re}(\text{CO})_3(\text{py})(\text{phen})]^+$ .<sup>38,39</sup> The PL band of 4 was blue-shifted, with respect to that of 3 (by ca. 30 nm, see Table 1), and showed the desired increase in lifetime and quantum yields (with  $\Phi_{\text{em}}$  increasing from 0.5% for 3 to 6.9% for 4 in aerated water solution).

**Synthesis and Characterization of Re-PhenISA Complex.** The reaction of complex 1 with PhenISA was performed under the same conditions as the model reaction (pH 5.5, 323 K). Spectroscopic monitoring (IR, <sup>1</sup>H NMR) showed that, also in this case, the reaction went to completion within 30 min, indicating that the phenanthroline ligands are not significantly sheltered within the entangled polymer and are easily accessible for the metal centers.

However, the large bandwidth of the  $\nu_{\text{CO}}$  bands of Re-PhenISA (much larger than that of the model compound 3; see Figure S6 in the Supporting Information) suggests that different coordination environments are present in the polymer. The position of the IR bands (shifted to lower wavenumbers, with respect to 3) agrees with the formation of neutral species,<sup>40</sup> in which the sixth coordination position around Re is occupied by an anionic ligand, most likely one of the carboxylate groups omnipresent along the polymer skeleton (see Chart 4a).

The polymeric complex was isolated by ultracentrifugation and elemental analysis of the retained fraction confirmed a 1:1 phenanthroline/ $\text{Re}(\text{CO})_3^+$  ratio. DLS measurements showed that the aggregation extent of the polymer chains was not modified by the presence of the metal ( $D_t = 23.8 (\pm 1.2) \mu\text{m}^2/\text{s}$ , corresponding to a hydrodynamic diameter  $d_H = 21 \pm 1$  nm).

In the UV-vis spectrum of Re-PhenISA, a relatively weak absorption band at ca. 360 nm (Figure 4) was detectable, which

**Table 1.** Spectroscopic and Photophysical Data for the Model Compounds 3 and 4 and for the Investigated Polymeric Complexes<sup>a</sup>

compound	IR $\nu(\text{CO})$ ( $\text{cm}^{-1}$ )	$\lambda_{\text{abs MLCT}} (\epsilon)$ (nm, $\text{cm}^{-1} \text{M}^{-1}$ )	$\lambda_{\text{em}}$ (nm)	$\Phi_{\text{em}} (\times 10^2)$	lifetime (ns)
$[\text{Re}(\text{CO})_3(\text{OH}_2)(\text{BAP})]^+$ (3)	2034, 1921	364 (3100)	597 <sup>b</sup>	0.5	40 (97%)
$[\text{Re}(\text{CO})_3(\text{py})(\text{BAP})]^+$ (4)	2035, 1929	366 (3300)	568 <sup>c</sup>	6.9	544 (97%)
Re-PhenISA	2025, 1910	362 (3500)	608 <sup>b</sup>	0.7	260 (55%) 40 (45%)
Re-Py-PhenISA	2034, 1930	364 (3800)	571 <sup>c</sup>	4.8	550 (98%)
Ru-PhenISA		430 (18 900), 458 (19 100)	614 <sup>d</sup>	4.1	580

<sup>a</sup>Conditions: in aerated water solution, room temperature, pH 5.5. <sup>b</sup> $\lambda_{\text{ex}} = 400$  nm. <sup>c</sup> $\lambda_{\text{ex}} = 375$  nm. <sup>d</sup> $\lambda_{\text{ex}} = 490$  nm.

Chart 4. Schematic Drawings of (a) the Re-PhenISA Copolymer, Showing the Coordination of a Carboxylate Anion to Complete the Coordination Sphere of Rhenium, and (b) the Re-Py-PhenISA Copolymer

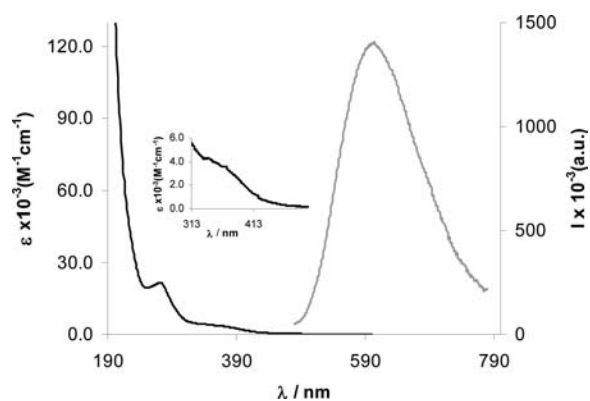
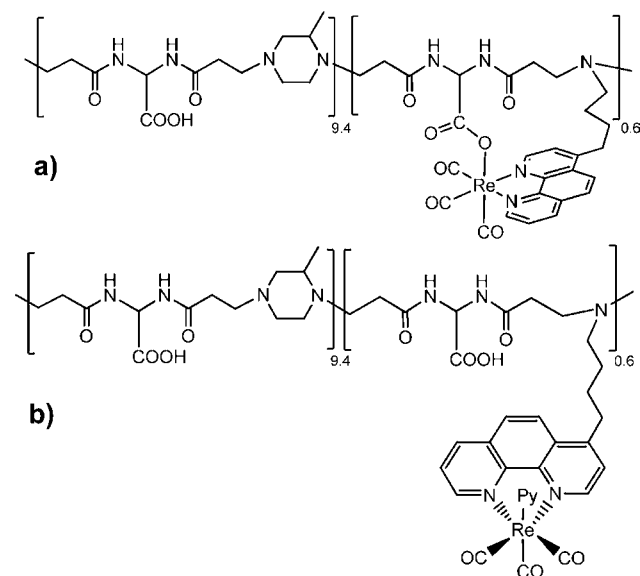


Figure 4. UV-vis absorption (left, black) and photoluminescence (PL) (right, gray,  $\lambda_{\text{ex}} = 400 \text{ nm}$ ) spectra of **Re-PhenISA** (inset shows a magnified view of the  $^1\text{MLCT}$  absorption band).

was due to the singlet metal-to-ligand charge transfer transition ( $^1\text{MLCT}$ ), typical of Re(I)-diimine complexes (see Table 1). Also typical of these compounds is the broad featureless emission band in the red region,<sup>9,10</sup> shown in Figure 4. Both the wavelength of the emission and the photoluminescence yields ( $\Phi_{\text{em}} = 0.7\%$  in aerated water) were comparable to those of many other neutral tricarbonyl diimine Re(I) emitters.<sup>10</sup> A biexponential decay of the excited states was observed (lifetimes  $\tau = 260$  and  $40 \text{ ns}$ , accounting for 55% and 45% of the emission, respectively). The short lifetime perfectly agrees with the value measured for the model aquo-derivative **3** (see Table 1), and with the value of  $28 \text{ ns}$  measured for an analogous aquo complex in ref 38.<sup>41</sup> This might be suggestive of the presence in the polymer, in addition to the main carboxylate derivative, as well as a minor amount of a complex bearing water in the sixth position. However, the observation of two lifetime values does not necessarily imply the presence of two species: multiexponential decay can arise from heterogeneity of the environment, particularly in macromolecular systems, either in solid film<sup>42</sup> or in solution.<sup>43</sup> Therefore, the

hypothesis that both lifetimes are due to the carboxylate derivative in a heterogeneous environment cannot be ruled out. Moreover, a biexponential decay, with very similar lifetime values ( $\tau = 244$  and  $31 \text{ ns}$ ), was measured for the  $[\text{Re}(\text{CO})_3(\text{OC}(\text{O})\text{CH}_3)(\text{bpy})]$  complex, in  $\text{CH}_2\text{Cl}_2$  solution.<sup>44</sup>

**Synthesis and Characterization of the Re-Py-PhenISA Complex.** The better emitting **Re-Py-PhenISA** polymer complex (Chart 4b) was prepared by using the reaction conditions established in the synthesis of model complex **4**. The reaction rate was lower than that in the synthesis of **4** (ca. 48 h, based on the IR monitoring, see Figure S8 in the Supporting Information, compared to 24 h for **4**). This is in agreement with the hypothesis that, in this case, the leaving group is an anionic species rather than a more labile water molecule. DLS measurements showed that the hydrodynamic diameter of the nanoparticles ( $23 \pm 1 \text{ nm}$ ) after pyridine insertion was unchanged compared with that of **Re-PhenISA**, suggesting that the polymer chain was not significantly degraded under the reaction conditions. This was confirmed by transmission electron microscopy (TEM) analysis, showing that **Re-Py-PhenISA** had a nanoparticulated structure with a size distribution histogram peaking at ca. 21 ppm (Figure 5). Similar results were obtained in the case of **PhenISA** and **Re-PhenISA** (data not shown).

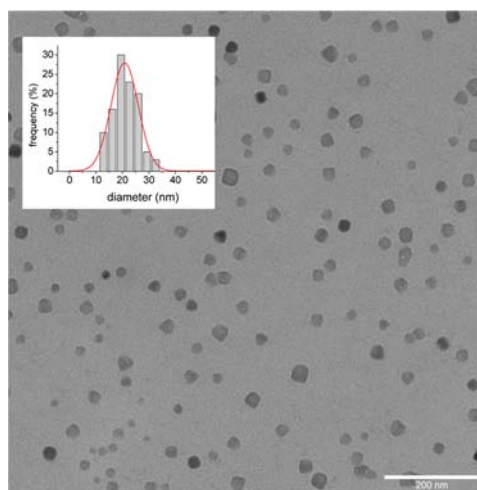
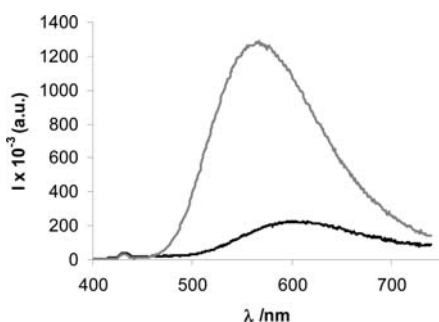


Figure 5. TEM micrograph of **Re-Py-PhenISA** and the relative size distribution histogram (the scale bar in the lower right-hand corner corresponds to 200 nm).

**Re-Py-PhenISA** exhibited spectroscopic properties very similar to those of **4** (see Table 1). Accordingly, with respect to **Re-PhenISA**, the emission maximum moved from 608 nm (orange) to 571 nm (bright yellow) and the quantum yields of the emission increased from 0.7% to 4.8% in aerated water solution (see Figure 6 and Table 1).

**Synthesis and Characterization of Ru-PhenISA.** Polypyridine Ru(II) complexes of the general formula  $[\text{Ru}(\text{N}^{\wedge}\text{N})_3]^{2+}$  (with  $\text{N}^{\wedge}\text{N} = \text{bipyridine}$  or  $\text{phenanthroline}$ ) are, by far, the most extensively investigated luminescent transition-metal complexes.<sup>45</sup> The MLCT excited states of such complexes have been exploited both in materials science (for instance, dyes for solar cells)<sup>46</sup> and in biological applications, such as staining specific cell compartments for in vivo imaging,<sup>4e,47</sup> or monitoring the behavior of active molecules in living species.<sup>48</sup> In particular, Ru complexes functionalized with suitable intercalating ligands have been used as probes of

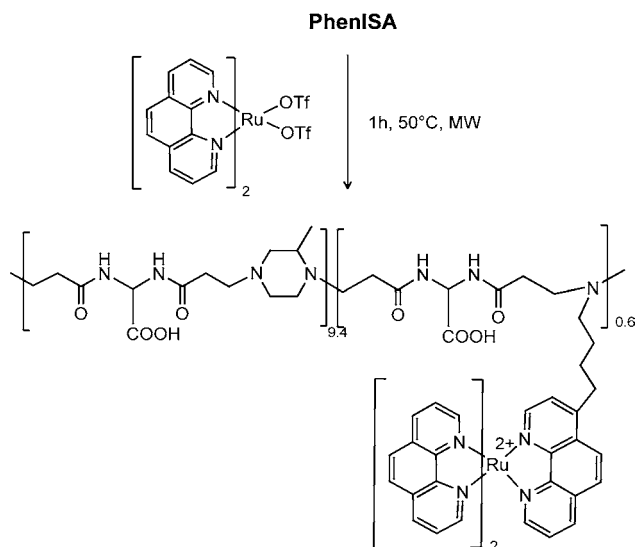


**Figure 6.** Photoluminescence (PL) spectra ( $\lambda_{\text{ex}} = 375$  nm) in aerated water of **Re-PhenISA** (black trace) and **Re-Py-PhenISA** (gray trace).

DNA structure,<sup>49</sup> able to act as smart molecular “light switch” agents.<sup>43</sup> Dendritic polyamidoamines<sup>26</sup> or polymeric vesicles<sup>50</sup> have sometimes been employed as carrier of Ru complexes, to improve and control their cellular uptake and also to increase their brightness.<sup>26</sup> Therefore, it was of interest to investigate the binding of a ruthenium polypyridyl moiety to the **PhenISA** carrier.

The **Ru-PhenISA** complex was prepared by reacting **PhenISA** with an equivalent amount (with respect to phenanthroline moieties) of the  $[\text{Ru}(\text{phen})_2(\text{CF}_3\text{SO}_3)_2]$  complex, in aqueous solution at 323 K, for 1 h using microwave activation (Scheme 2). The reaction progress was monitored by

#### Scheme 2. The Synthesis of **Ru-PhenISA**<sup>a</sup>



<sup>a</sup>MW = microwave.

UV-vis and the resultant orange **Ru-PhenISA** complex was purified by ultracentrifugation. The <sup>1</sup>H NMR spectrum (see Figure S9 in the Supporting Information) was in agreement with the proposed structure. Resonance peaks were assigned by scalar and dipolar 2D NMR spectra, following spectral data reported for the  $[\text{Ru}(\text{phen})_3]^{2+}$  complex.<sup>51</sup> Inductively coupled plasma (ICP) analysis confirmed that the amount of bound ruthenium was very close (93%) to the maximum loading. The hydrodynamic diameter obtained by DLS was  $18 \pm 2$  nm, which is very close to that observed for **PhenISA** and the Rhenium containing analogues.

The photophysical properties of **Ru-PhenISA** (see Table 1 and Figure 7) are very similar to those of conventional

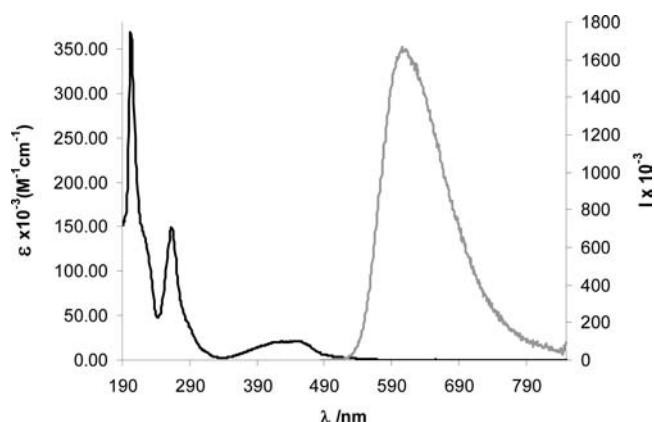


**Figure 7.** UV-vis absorption spectrum (black) and PL spectrum (gray,  $\lambda_{\text{ex}} = 490$  nm) of **Ru-PhenISA**.

$[\text{Ru}(\text{phen})_3]^{2+}$  complexes.<sup>52</sup> The UV-vis absorption spectrum showed the typical MLCT transition at ca. 450 nm, and in the PL spectrum, an emission centered at 614 nm was observed, with a lifetime of 580 ns and  $\Phi_{\text{em}} = 4.1\%$ , in aerated water solution.

**Stability under Physiological Conditions, Cell Toxicity, and Cellular Uptake.** The stability of the three complexes **Re-PhenISA**, **Re-Py-PhenISA**, and **Ru-PhenISA** under physiological conditions (pH 7.4, 0.15 M NaCl) in the presence of excess cysteine (20 equiv, with respect to Re or Ru) was evaluated by monitoring the variation of the absorption and emission spectra over time. No significant change was observed over 24 h (as shown in Figure S10 in the Supporting Information for the Ru complex), thus indicating that the interaction of the  $\text{Re}(\text{CO})_3$  or  $\text{Ru}(\text{phen})_2$  fragments with the phenanthroline ligand on the polymer is sufficiently strong to avoid cleavage of the metal-polymer interaction, even in the presence of a large excess of strong potential external ligands, such as cysteine. As expected, cysteine is not able to break the M-phen bond. Nevertheless, it is noteworthy that, despite the strong affinity of Re toward S-donor ligands, cysteine was not able to coordinate the sixth position of the  $\text{Re}(\text{CO})_3$  moiety.<sup>24</sup>

To test a possible toxic effects of the metal complexes, HEK-293 cells were incubated for 24 h with three different concentrations of **Re-Py-PhenISA** and **Ru-PhenISA**, namely, the standard concentration used for the cell uptake experiments described below ( $5 \mu\text{M}$ ) and 10-fold higher ( $50 \mu\text{M}$ ) or lower ( $0.5 \mu\text{M}$ ) concentrations. None of the polymer complexes provided evidence of toxic effect on the cells, even at the highest concentration, as shown in the bar diagram of Figure S11 in the Supporting Information.

Finally, a preliminary investigation of cell internalization and intracellular distribution was performed, by means of fluorescence confocal microscopy. **Ru-PhenISA** was used for this study, since its absorption spectrum ( $458$  nm, see Table 1) is consistent with the wavelength of the excitation source available on the instrument ( $450$  nm). HEK-293 cells were incubated with **Ru-PhenISA** (see Experimental Section) and analyzed after 6 and 12 h. After 6 h, most of the complex localized in vesicular compartments within the cytoplasm (Figure 8a), suggesting an active pathway for cell internalization, such as endocytosis or micropinocytosis, whereas after 12 h (Figure 8b), the complex appeared to be almost homogeneously distributed inside the cytoplasm, indicating subsequent complex escape across the vesicular membrane. The

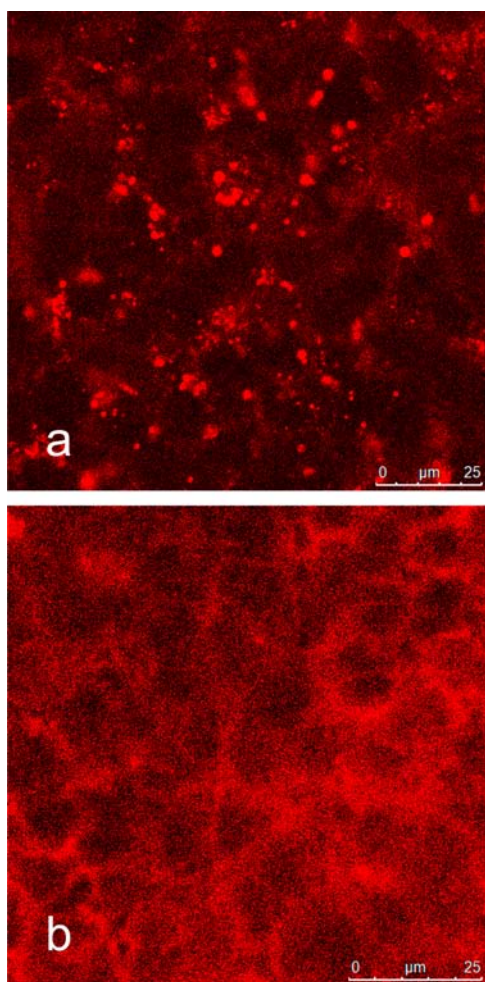


**Figure 8.** Confocal microscopy images of HEK-293 cells incubated with Ru-PhenISA (ca. 5  $\mu\text{M}$ ) for (a) 6 h and (b) 12 h. Field of view is 111  $\mu\text{m} \times 111 \mu\text{m}$  for panel (a) and 89  $\mu\text{m} \times 89 \mu\text{m}$  for panel (b). Figure S12 in the Supporting Information shows the corresponding bright-field images and their merge with the luminescence images.

ability of PAAs to permeabilize endocytic vesicular membranes in response to reducing the pH inside the organelle, with consequent delivery of the vesicle content, was previously demonstrated both in vitro and in vivo.<sup>22,53</sup>

## CONCLUSIONS

The insertion of phenanthroline ligands into the skeleton of an amphoteric PAA was successfully achieved. The resultant PhenISA copolymer, which was endowed with the same excellent water solubility as ISA23, stably coordinated both rhenium and ruthenium pro-luminescent complexes. The polymeric derivatives so obtained exhibited photophysical properties that are almost superimposable to those of the corresponding molecular complexes, suggesting that binding to the macromolecular chain did not affect the interaction of the metal centers with the environment. On the other hand, the metal-PhenISA complexes maintained the nanometric size, water solubility, and biocompatibility of parent PhenISA. Therefore, conjugates joining the favorable properties of PAAs and of the selected transition-metal complexes were obtained, thus opening the pathway to several future improvements.

In fact, the properties of the nanoconjugates described here appear widely tunable. It would be possible to modulate the

wavelength, lifetime, and intensity of the emission by changing the substituents on the phenanthroline or the metal itself. It will also be possible to vary the size of the polymer or the number of phenanthroline ligands on the macromolecule, by varying the conditions of the copolymerization reaction. The structure of the PAA main chain can also be varied, in order to tune the cell internalization and intracellular trafficking. The preliminary cellular uptake experiments here described already suggested that the metal-PhenISA complexes enter cells by endocytic pathway and, subsequently, homogeneously diffuse within the cytoplasm across the vesicle membranes. This behavior resembles that of the polymeric vesicles (polymersomes), developed by Battaglia and co-workers, as biomimetic nano-vectors,<sup>50,54</sup> which are able to enter cells by endocytosis and then escape via the endocytic pathway to release their content (bioactive agents) within the cells. The development of PhenISA-based systems toward similar applications can be envisaged.

Last, but not least, an important potentiality of the Re-PhenISA conjugates should be considered. Rhenium possesses two radioisotopes (<sup>188</sup>Re and <sup>186</sup>Re), both of which, because of their  $\beta^-$  and  $\gamma$  emissions, have potential applications in cancer therapy and diagnosis, respectively. The preparation of  $[\text{Re}(\text{CO})_3(\text{OH}_2)_3]^+$  (**1**) samples incorporating radioactive Re isotopes is well-established,<sup>37,55</sup> and the reaction of **1** with PhenISA is fast enough to be compatible with the lifetimes of both rhenium radioisotopes (17 h for <sup>188</sup>Re, 88 h for <sup>186</sup>Re). Therefore, in principle, it is possible to develop a bimodal theranostic system, endowed with rhenium complexes able to act both as dyes for optical imaging and as  $\gamma$  emitters for radio-imaging, with the additional benefit of  $\beta^-$ -emission for therapy. Such dual systems are of high interest,<sup>56</sup> because they combine the high spatial resolution of fluorescence microscopy, useful for both in vitro and ex vivo studies, with the accurate localization, deep within the body, of radioactive probes in vivo, bridging the gap between such different imaging approaches.<sup>57</sup> The Re-PhenISA system presented here has the potential for dual-modality-imaging based on a single compound, obtained with a single preparation step.<sup>58</sup>

## EXPERIMENTAL SECTION

**Materials.** Ultrapure water (Milli-Q, Millipore, resistivity = 18 M $\Omega$  cm<sup>-2</sup>) was used for the preparation of the aqueous solutions. D<sub>2</sub>O (99.9%) was purchased from Aldrich and used as received. 2-Methylpiperazine was purchased from Fluka and used after sublimation. Its final purity (98%) was determined with acidimetric titration. *N,N'*-Bis(acrylamido)acetic acid (BAC) was prepared as reported in the literature,<sup>59</sup> and purity (98%) was determined by NMR spectroscopy and titration. Re<sub>2</sub>(CO)<sub>10</sub> was purchased from Sigma-Aldrich and used as received. Re(CO)<sub>5</sub>Br,<sup>60</sup> Re(CO)<sub>5</sub>(CF<sub>3</sub>SO<sub>3</sub>),<sup>61</sup> and [Re(CO)<sub>3</sub>(OH<sub>2</sub>)<sub>3</sub>](CF<sub>3</sub>SO<sub>3</sub>),<sup>62</sup> were synthesized according to literature procedures (slightly modified in the latter case by the addition of a small amount of CF<sub>3</sub>SO<sub>3</sub>H before refluxing; see ref 24). [Ru(phen)<sub>2</sub>Cl<sub>2</sub>] and [Ru(phen)<sub>2</sub>(CF<sub>3</sub>SO<sub>3</sub>)<sub>2</sub>] were prepared using the methods employed for the synthesis of [Ru(bpy)<sub>2</sub>Cl<sub>2</sub>]<sup>63</sup> and [Ru(bpy)<sub>2</sub>(CF<sub>3</sub>SO<sub>3</sub>)<sub>2</sub>],<sup>64</sup> respectively. All the other reagents were purchased from Aldrich and used as received, without further purifications, if not otherwise specified. THF was dried using the M. Braun SPS-800 solvent purification system. CH<sub>2</sub>Cl<sub>2</sub> was distilled from P<sub>4</sub>O<sub>10</sub> using standard Schlenk techniques.

**Instruments and Methods.** NMR experiments were performed on a Bruker Model DRX400 spectrometer (operating at 400.13, 100.62, and 40.55 MHz for <sup>1</sup>H, <sup>13</sup>C, and <sup>15</sup>N NMR, respectively), equipped with a Bruker 5 mm BBI Z-gradient probe head capable of producing gradients with a strength of 53.5 G/cm. <sup>15</sup>N NMR spectra



were referenced to external  $\text{CH}_3\text{NO}_2$ . All spectra were acquired at 300 K using standard 1D and 2D NMR experiments on samples typically containing 10–30 mg of lyophilized polymer samples dissolved in 500  $\mu\text{L}$  of  $\text{D}_2\text{O}$  (or of a  $\text{D}_2\text{O}/\text{H}_2\text{O}$  1/9 mixture, when necessary to identify the NH protons). The  $\pi/2$  pulse lengths were 6.9  $\mu\text{s}$  ( $^1\text{H}$ ), 9.25  $\mu\text{s}$  ( $^{13}\text{C}$ ), and 31.0  $\mu\text{s}$  ( $^{15}\text{N}$ ). The DOSY maps of Figure 1 and Figure S1 in the Supporting Information were obtained by a  $^1\text{H}$  pulsed-field-gradient spin echo (PGSE) NMR experiment (not calibrated), performed at room temperature. A stimulated echo sequence (STE)<sup>65</sup> incorporating bipolar gradient pulses, was used,<sup>66</sup> with water suppression for the experiment of Figure 1 (standard Bruker pulse programs *stebppg1s19*). The gradient strength ( $G$ ) was linearly incremented in 16 steps from 5% to 95% of its maximum value. A diffusion time of  $\Delta = 500$  ms and a gradient pulse duration of  $\delta = 4$  ms were used.

Infrared (IR) spectra were acquired on a Bruker Model Vector 22 FT instrument, using 0.1 mm  $\text{CaF}_2$  cells. Electronic absorption spectra were recorded on an Agilent Model 8543 spectrophotometer at room temperature. Steady-state photoluminescence (PL) measurements were performed on a Jobin-Yvon–Horiba Fluorolog spectrometer and emission spectra were corrected for the spectroscopic sensitivity of the photomultiplier tube. Quantum yields were determined by comparison with the emission of  $[\text{Ru}(\text{bpy})_3]\text{Cl}_2$  for the metal complexes ( $\Phi_{\text{em}} = 0.04$  in aerated water), and with the emission of quinine bisulfate for PhenISA ( $\Phi_{\text{em}} = 0.52$  in 1 N  $\text{H}_2\text{SO}_4$ ).<sup>67</sup>

Dynamic fluorescence measurements were performed with a frequency-modulated phase fluorometer (Digital K2, ISS, Inc., Urbana, IL). The excitation was accomplished by the 9-mW output of a 378-nm diode laser (ISS, Inc., Urbana, IL). At least 15 data points at logarithmically spaced frequencies in the range 0.3–30 MHz with a cross-correlation frequency of 400 Hz (Model A2D, ISS, Inc., USA) were acquired for lifetime measurements. The convenient accuracy for phase angles and modulation ratios was  $0.2^\circ$  and 0.004, respectively. Lifetime measurements were performed under the magic-angle condition,<sup>68</sup> and a 535-nm long-pass filter (Andover Co.) was employed in order to reduce light scattering. A solution of glycogen in doubly distilled water was used as a reference sample.<sup>69</sup> Lifetime data fitting was accomplished by an ISS routine based on the Marquardt least-squares minimization, with at least two exponential components in the decay scheme in order to take into account the scattering contribution to the overall signal. The fit of the fluorescence intensity decay  $F(t)$  yields the lifetime values,  $\tau_i$ , together with the corresponding fractional intensities  $f_i$ :

$$F(t) = \sum \alpha_i e^{-t/\tau_i}$$

and

$$f_i = \frac{\alpha_i \tau_i}{\sum \alpha_i \tau_i}$$

where  $\alpha_i$  represent the pre-exponential factors.

The optical confocal setup employed to study the cellular uptake of Ru-PhenISA by HEK-293 cells was a Leica TCS resonant STED DMI6000 CS microscope equipped with a multiline  $\text{Ar}^+$  laser, two highly efficient hybrid detectors, and highly sensitive prism spectral detectors.

Elemental C, H, N analyses were performed on a Perkin–Elmer CHN 2400 instrument, while the metal content was determined by ICP analysis on a Perkin–Elmer Optima 8300 instrument.

Ultrafiltration for the purification of the synthesized polymers was performed using an Amicon apparatus through a membrane with a nominal cutoff of 1000 or 3000 Da. The purification of the polymeric rhenium complexes was performed either by ultracentrifugation or dialysis. Ultracentrifugations were performed on a Beckman Model J2-21 centrifuge equipped with a Model JA-20 35° fixed-angle rotor, using Amicon Ultra-4 or Centricon centrifugal filter devices (Millipore) with 3000 nominal molecular weight limit (NMWL) membranes. The solutions were diluted up to 1:10, and centrifugation processes were repeated until the IR spectrum of the filtrate (concentrated to a small volume, ca. 100  $\mu\text{L}$ ) did not show any absorption attributable to

$\text{Re}(\text{CO})_3$  fragments. Dialysis processes were performed using 12–14 kDa cutoff membranes (Spectrapore) against ultrapure water.

Size exclusion chromatography (SEC) traces were obtained with Toso-Haas TSK-gel G4000 PW and TSK-gel G3000 PW columns connected in series, using a Waters model 515 HPLC pump equipped with a Knauer autosampler 3800, a light scattering and viscometer Viscotek 270 dual detector, UV detector Waters model 486 operating at 230 nm, and a refractive index detector (Waters, Model 2410). The mobile phase was a 0.1 M Tris buffer (pH  $8.00 \pm 0.05$ ) with 0.2 M sodium chloride. The flow rate was 1  $\text{mL min}^{-1}$ , and the sample concentration was 1% (w/w).

DLS measurements were performed on a Malvern Zetasizer nano ZS instrument at 298 K on diluted samples (1 mg/mL) in ultrapure water at various pH. Standard deviations of the diffusion coefficients were obtained by the nonlinear fitting of the correlation function<sup>70</sup>

$$G(t) = 0.15 \left( \sum_i A_i e^{-D_i q t} \right)^2$$

where  $q$  is the wave vector ( $q = 4\pi n / [\lambda \sin(\theta/2)]$ ),  $\lambda$  the wavelength of the incident light ( $\lambda = 633$  nm),  $\theta$  the detecting angle ( $\theta = 173^\circ$ ), and  $n$  the refractive index of the solution approximated to that of the pure solvent ( $n = 1.33$ ). The standard deviations of the hydrodynamic diameters were computed accordingly using the Origin data analysis software package. From the diffusion coefficients, the hydrodynamic diameter ( $d_H$ ) is obtained through the Stokes–Einstein equation,

$$D_i = \frac{kT}{c\pi\eta r_H}$$

where  $k$  is the Boltzmann's constant,  $T$  the absolute temperature,  $\eta$  the solution viscosity (approximated to that of pure water), and  $c$  a factor that is dependent on the size of the diffusing species (with  $c$  ranging in value between 4 (slip boundary conditions) and 6 (stick boundary conditions)).<sup>71</sup>

**Preparation of Complex ISA23SH-[Re(CO)<sub>3</sub>(BPS)] (BPS = Bathophenanthroline Sulfonate).** At first, the  $[\text{Re}(\text{CO})_3(\text{OH}_2)]^+$  (BPS)<sup>−</sup> complex **2** was prepared by reacting 1 mL of a 0.1 M solution of the aquo complex **1** with stoichiometric BPS (69.5 mg, 0.1 mmol), at 353 K for 24 h. The solution color progressively turned to yellow, and the final IR spectrum of **2** showed  $\nu(\text{CO})$  bands at 2033(s) and 1926(vs)  $\text{cm}^{-1}$ . UV–vis ( $\text{H}_2\text{O}$ ):  $\lambda_{\text{max}} = 372$  nm; photoluminescence (aerated  $\text{H}_2\text{O}$  solution):  $\lambda_{\text{max}} = 615$  nm,  $\Phi_{\text{em}} = 0.5\%$ . The  $^1\text{H}$  NMR spectrum was strongly dependent on the pH and concentration of the solution (data not shown). The Re-ISA23SH complex was then prepared as follows: a copolymer ISA23SH solution (28.3 mg) in  $\text{H}_2\text{O}$  (2 mL) (5.0 mM cysteamine content) was treated with a slight defect (with respect to SH groups) of the complex **2** solution (86  $\mu\text{L}$ ) and the pH was adjusted to 5.5 with NaOH. The solution was heated at 353 K for 5 h and maintained for an additional 16 h at room temperature to complete the reaction. The color changed from yellow to deep orange, and the position of the  $\nu(\text{CO})$  IR bands moved to 2024(s) and 1919(vs)  $\text{cm}^{-1}$ . To remove the possible presence of unreacted free **2**, the reaction mixture was diluted 1:20 with water and ultracentrifuged (5000 rpm, 293 K, 5 cycles, 1 h each), until no  $\nu(\text{CO})$  bands were detected in the filtrates. Finally, the retained portions were lyophilized. Yield: 20.8 mg (57%). UV–vis ( $\text{H}_2\text{O}$ ):  $\lambda_{\text{max}} = 376$  nm; photoluminescence (aerated  $\text{H}_2\text{O}$  solution):  $\lambda_{\text{max}} = 629$  nm,  $\Phi_{\text{em}} = 0.4\%$ . A stability assay was performed on a sample of ISA23SH-[Re(CO)<sub>3</sub>(BPS)] (5 mM with respect to the Re content) dissolved in a saline solution (0.15 M NaCl) at pH 7.4. The addition of 20 equiv of cysteine (with respect to Re) resulted in cleavage of the Re–polymer bond, after 24 h of interaction at room temperature, as revealed by the IR analysis of the filtrates after ultracentrifugation.

**Synthesis of 4-(4'-Aminobutyl)-1,10-phenanthroline (BAP).** The amino-functionalized phenanthroline BAP was prepared by a slightly modified literature procedure.<sup>33</sup> To a lithium diisopropylamide (LDA) solution (1.06 mmol) in anhydrous THF (2.2 mL), a sample of 4-methyl-1,10-phenanthroline (200 mg, 0.999 mmol) dissolved in anhydrous THF (6.6 mL) was slowly added at 195 K. The solution

turned instantaneously dark brown. The mixture was then warmed to room temperature and subjected to stirring for 12 h. 1-(3-Bromopropyl)-2,2,5,5-tetramethyl-1-aza-2,5-disilacyclopentane (1 mmol) dissolved in THF (660  $\mu\text{L}$ ) was added, and the mixture stirred for 4 days.

The solution turned from dark brown to dark green with the formation of a precipitate. The reaction was quenched by adding a  $\text{KHCO}_3$  saturated aqueous solution (3.5 mL) and a 15% NaOH solution (3.3 mL). The aqueous phase then was extracted with THF (3  $\times$  10 mL), and the organic layers collected and vacuum-dried. The crude product was treated with 1 M HCl and stirred for 3 h to deprotect the amine group, then treated with concentrated NaOH to adjust the pH at ca. 6. Maintaining this pH, unreacted 4-methyl-1,10-phenanthroline, together with silane byproducts derived from the amine group deprotection, were successfully eliminated by repeated extractions with  $\text{CH}_2\text{Cl}_2$  (5  $\times$  5 mL). The aqueous phase was then vacuum-dried, and the wet solid was treated with anhydrous  $\text{Et}_2\text{O}$  several times to remove hydrogen-bonded water, eventually obtaining an other solid. Yield: 137 mg (54%).  $^1\text{H}$  NMR ( $\text{H}_2\text{O}/\text{D}_2\text{O}$  9:1, pH 10)  $\delta$  1.37–1.49 (4H,  $\text{CH}_2(b)$  and  $\text{CH}_2(c)$ , m), 2.57–2.68 (4H,  $\text{CH}_2(a)$  and  $\text{CH}_2(d)$ , m), 7.21 (1H, H3, d,  $J$  = 4.6 Hz), 7.30 (1H, H6, d,  $J$  = 9.1 Hz), 7.42 (1H, H5, d,  $J$  = 9.1 Hz), 7.51 (1H, H8, dd,  $J$  = 4.4, 8.1 Hz), 7.99 (1H, H7, dd,  $J$  = 1.5, 8.1 Hz), 8.62 (1H, H2, d,  $J$  = 4.6 Hz), 8.82 (1H, H9, dd,  $J$  = 1.5, 4.4 Hz).

**Synthesis of the Copolymer PhenISA.** To a solution of BAC (394 mg, 1.95 mmol) and NaOH (79.2 mg, 1.98 mmol, pH 9–10) in water (640  $\mu\text{L}$ ), 4-(4'-aminobutyl)-1,10-phenanthroline (50.2 mg, 0.194 mmol, 97% purity from  $^1\text{H}$  NMR analysis) was added. The reaction was left for 48 h at room temperature under gentle stirring, then 2-methylpiperazine was added (184 mg, 0.174 mmol). The mixture was maintained under the same conditions for an additional 5 days, during which the viscous solution turned from light yellow to honey-colored. After this period, the crude reaction mixture was diluted with water (10 mL) and acidified to pH 3 by the addition of few drops of triflic acid. The solution was purified by ultrafiltration through a membrane with a nominal cutoff of 3000 Da and the retained portion was recovered by freeze-drying. Yield: 620 mg (70%).  $M_n$  = 46 790,  $M_w$  = 83 100, PD = 1.78. The polymer contained variable amounts of the triflate anion, as revealed by  $^{19}\text{F}$  NMR and elemental analysis.  $^1\text{H}$ ,  $^{13}\text{C}$ , and  $^{15}\text{N}$  NMR ( $\text{D}_2\text{O}$ , 9:1, pH 3.2) results are reported in Table S1 in the Supporting Information. The loading of BAP (6% on a molar basis) was estimated by  $^1\text{H}$  NMR. Elemental analysis: Found = C, 39.24; H, 6.61; N, 12.95; C/N = 3.03 (calcd for  $(\text{C}_{13}\text{H}_{22}\text{N}_4\text{O}_4)_{0.94}(\text{C}_{24}\text{H}_{27}\text{N}_3\text{O}_4)_{0.06}(\text{CF}_3\text{SO}_3\text{H})_{0.6}(\text{H}_2\text{O})_2$ : C, 39.51; H, 6.25; N, 13.12; C/N = 3.01).

**Preparation of the Model Complex  $[\text{Re}(\text{CO})_3(\text{OH}_2)(\text{BAP})](\text{CF}_3\text{SO}_3)$  (3).** A sample of  $[\text{Re}(\text{CO})_3(\text{OH}_2)_3]\text{CF}_3\text{SO}_3$  (1) (200  $\mu\text{L}$  of a 0.1 M solution) was added to 1 mL of a 0.02 M aqueous solution of BAP. The pH was immediately adjusted to 5.5 by the addition of few drops of 1 M NaOH, and the mixture heated at 323 K for 30 min. IR  $\nu(\text{CO})$ ,  $\text{H}_2\text{O}$  solution: 2034(s) and 1921(s)  $\text{cm}^{-1}$ .  $^1\text{H}$  NMR ( $\text{D}_2\text{O}$ , pH 5; for the assignment of the BAP positions, see Chart S1 in the Supporting Information):  $\delta$  1.73 (2H,  $\text{CH}_2(b)$ , q,  $J$  = 7.5), 1.83 (2H,  $\text{CH}_2(c)$ , q,  $J$  = 7.5), 2.99 (2H,  $\text{CH}_2(a)$  pseudo, t,  $J$  = 7.5 Hz), 3.20 (2H,  $\text{CH}_2(d)$ , m), 7.75 (1H, H3, d,  $J$  = 5.5 Hz), 7.92 (1H, H8, dd,  $J$  = 8.3, 5.2 Hz), 7.99 (1H, H6, d,  $J$  = 9.2 Hz), 8.14 (1H, H5, d,  $J$  = 9.2 Hz), 8.67 (1H, H7, dd,  $J$  = 8.5, 0.9 Hz), 9.25 (1H, H2, d,  $J$  = 5.3 Hz), 9.40 (1H, H9, dd,  $J$  = 4.8, 0.9 Hz).  $^{13}\text{C}$  NMR ( $\text{D}_2\text{O}$ , pH 5):  $\delta$  26.3 ( $\text{CH}_2(b)$  and  $\text{CH}_2(c)$ ), 31.0 ( $\text{CH}_2(d)$ ), 39.1 ( $\text{CH}_2(a)$ ), 123.6 ( $\text{CH}(5)$ ), 125.8 ( $\text{CH}(3)$ ), 125.9 ( $\text{CH}(8)$ ), 127.2 ( $\text{CH}(6)$ ), 139.8 ( $\text{CH}(7)$ ), 153.4 ( $\text{CH}(2)$ ), 154.1 ( $\text{CH}(9)$ ).

**Reaction of the Model Complex  $[\text{Re}(\text{CO})_3(\text{OH}_2)(\text{BAP})]^+$  with Acetate Ions.** A  $1.7 \times 10^{-2}$  M water solution (450  $\mu\text{L}$ ) of complex 3 was treated with  $\text{CH}_3\text{COONa}$  (3 mg) and heated at 333 K overnight. A yellow precipitate formed, which was isolated and dissolved in EtOH. IR  $\nu(\text{CO})$  (EtOH): 2025(s), 1919(s), and 1904(sh)  $\text{cm}^{-1}$ .  $^1\text{H}$  NMR ( $\text{DMSO}-d_6$ ; for the assignment of the BAP positions, see Chart S1 in the Supporting Information):  $\delta$  1.70 (2H,  $\text{CH}_2(b)$ , m), 1.84 (2H,  $\text{CH}_2(c)$ , m), 1.92 (3H,  $\text{CH}_3$ , s), 2.89 (2H,  $\text{CH}_2(a)$ , m), 3.34 (2H,  $\text{CH}_2(d)$ , m), 7.96 (1H, H3), 8.11 (1H, H8), 8.36 (1H, H6), 8.49 (1H,

H5), 8.97 (1H, H7), 9.32 (1H, H2), 9.44 (1H, H9).  $^{13}\text{C}$  NMR ( $\text{DMSO}-d_6$ ):  $\delta$  21.3 ( $\text{CH}_3$ ), 26.9 ( $\text{CH}_2(c)$ ), 27.0 ( $\text{CH}_2(b)$ ), 31.2 ( $\text{CH}_2(d)$ ), 38.9 ( $\text{CH}_2(a)$ ), 124.6 ( $\text{CH}(5)$ ), 126.2 ( $\text{CH}(3)$ ), 126.7 ( $\text{CH}(8)$ ), 127.8 ( $\text{CH}(6)$ ), 139.6 ( $\text{CH}(7)$ ), 153.6 ( $\text{CH}(2)$ ), 154.4 ( $\text{CH}(9)$ ).

**Preparation of the Model Complex  $[\text{Re}(\text{CO})_3(\text{py})(\text{BAP})](\text{CF}_3\text{SO}_3)$  (4).** A  $8.0 \times 10^{-3}$  M water solution (880  $\mu\text{L}$ ) of the complex  $[\text{Re}(\text{CO})_3(\text{OH}_2)(\text{BAP})](\text{CF}_3\text{SO}_3)$  (3) was treated with pyridine (11  $\mu\text{L}$ , ca. 20 equiv). A yellow precipitate immediately formed, likely constituted by the neutral complex  $[\text{Re}(\text{CO})_3(\text{OH})(\text{BAP})]$ . The precipitate was dissolved upon the addition of a few drops of  $\text{CF}_3\text{SO}_3\text{H}$ , until pH 5.5 was reached. The reaction mixture was heated at 323 K for 24 h. IR  $\nu(\text{CO})$  ( $\text{H}_2\text{O}$ , pH 5): 2034 and 1929  $\text{cm}^{-1}$ .  $^1\text{H}$  NMR ( $\text{D}_2\text{O}$ , pH 5; for the assignment of the BAP positions, see Chart S1 in the Supporting Information):  $\delta$  1.79 (2H,  $\text{CH}_2(b)$ , m), 1.72 (2H,  $\text{CH}_2(c)$ , m), 2.95 (2H,  $\text{CH}_2(a)$  pseudo, t,  $J$  = 7.1 Hz), 3.25 (2H,  $\text{CH}_2(d)$ , m), 7.86 (1H, H3, d,  $J$  = 5.5 Hz), 7.98 (1H, H8, dd,  $J$  = 8.5, 5.1 Hz), 8.05 (1H, H6, d,  $J$  = 9.2 Hz), 8.21 (1H, H5, d,  $J$  = 9.2 Hz), 8.70 (1H, H7, dd,  $J$  = 8.5, 0.8 Hz), 9.43 (1H, H2, d,  $J$  = 5.5 Hz), 9.55 (1H, H9, dd,  $J$  = 5.1, 0.8 Hz).

**Synthesis of Re-PhenISA Complex.** A sample of the PhenISA copolymer (30.5 mg,  $4.1 \times 10^{-3}$  mmol of BAP) was dissolved in water (1.5 mL) and the pH adjusted to 5.5 via the addition of 1 M NaOH. A 0.1 M solution of the aquo complex  $[\text{Re}(\text{CO})_3(\text{OH}_2)_3]\text{CF}_3\text{SO}_3$  (1) (45  $\mu\text{L}$ ,  $4.5 \times 10^{-3}$  mmol) then was added and the reaction mixture was heated at 323 K for 30 min under  $\text{N}_2$ . The solution color progressively turned from pale pink to honey yellow, while under UV irradiation orange luminescence was observed. The IR spectrum showed that the  $\nu(\text{CO})$  bands of the starting material (2037(s) and 1916(vs)  $\text{cm}^{-1}$ ) were replaced by new bands at 2025(s) and 1910(s)  $\text{cm}^{-1}$ . After ultracentrifugation (20 min at 7000 rpm, with a 3000 Da cutoff filter, 295 K), the IR spectrum of the retained fraction showed the  $\nu(\text{CO})$  bands of Re-PhenISA, whereas no CO bands were detectable in the IR spectrum of the filtrate. The retained fraction was lyophilized, affording a light yellow and fluffy material. Elemental analysis: Found = C, 47.50; H, 6.93; N, 16.16; Re 2.97% (calcd for  $(\text{C}_{13}\text{H}_{22}\text{N}_4\text{O}_4)_{0.94}(\text{C}_{28}\text{H}_{27}\text{F}_3\text{N}_3\text{O}_{16}\text{SRe})_{0.06}(\text{H}_2\text{O})$  C, 47.62; H, 6.99; N, 16.22; Re 3.19); Found C/N, 2.93 (calcd C/N, 2.94). The  $^1\text{H}$  and  $^{13}\text{C}$  NMR signals of the PAA backbone were indistinguishable from those of PhenISA (reported in Table S1 in the Supporting Information). NMR data of the phenanthroline pendant ( $\text{H}_2\text{O}/\text{D}_2\text{O}$  9:1, pH 5.5; for the assignment of the BAP positions, see Chart S1 in the Supporting Information):  $^1\text{H}$  NMR  $\delta$  1.87 ( $\text{CH}_2(b)$  and  $\text{CH}_2(c)$ , m), 3.16 ( $\text{CH}_2(a)$ , m), 3.33 ( $\text{CH}_2(d)$ , m), 7.83 (H3), 7.95 (H8), 8.14 (H6), 8.30 (H5), 8.75 (H7), 9.29 (H2), 9.39 (H9);  $^{13}\text{C}$  NMR:  $\delta$  22.8, 26.2 ( $\text{CH}_2(b)$  and  $\text{CH}_2(c)$ ), 30.9 ( $\text{CH}_2(d)$ ), 54 ( $\text{CH}_2(a)$ ), 123.8 ( $\text{CH}(5)$ ), 125.8 ( $\text{CH}(3)$ ), 125.9 ( $\text{CH}(8)$ ), 127.4 ( $\text{CH}(6)$ ), 139.5 ( $\text{CH}(7)$ ), 153.5 ( $\text{CH}(2)$ ), 154.0 ( $\text{CH}(9)$ ).

**Synthesis of the Re-Py-PhenISA Complex.** A water solution of Re-PhenISA complex (2.9 mL,  $5 \times 10^{-3}$  M, with respect to the BAP content) was treated with 20 equiv of pyridine (23  $\mu\text{L}$ ). The pH was set to 5.5 via the addition of few drops of triflic acid and the mixture was heated, under  $\text{N}_2$  at 323 K, for 48 h until disappearance of the  $\nu(\text{CO})$  IR bands of the starting material (replaced by absorptions at 2034 and 1930  $\text{cm}^{-1}$ ). The emitted light under UV lamp changed from orange to yellow. The pyridine excess was removed by dialysis against water (membrane cutoff 12–14 kDa). The retained fraction was lyophilized, affording a fluffy light yellow material. Elemental analysis: Found = C, 45.39; H, 7.53; N, 15.33; Re, 2.91%; C/N, 2.96 (calcd for  $(\text{C}_{13}\text{H}_{22}\text{N}_4\text{O}_4)_{0.94}(\text{C}_{33}\text{H}_{32}\text{N}_6\text{F}_3\text{O}_{16}\text{SRe})_{0.06}(\text{H}_2\text{O})_{2.0}$  C, 45.68; H, 7.18; N, 15.46; Re, 2.99%; C/N, 2.95). The  $^1\text{H}$  and  $^{13}\text{C}$  NMR signals of the PAA backbone were indistinguishable from those of PhenISA (reported in Table S1 in the Supporting Information). NMR data of the phenanthroline pendant ( $\text{H}_2\text{O}/\text{D}_2\text{O}$  9:1, pH 5.5; for the assignment of the BAP positions, see Chart S1 in the Supporting Information):  $^1\text{H}$  NMR  $\delta$  1.80 ( $\text{CH}_2(b)$  +  $\text{CH}_2(c)$ , m), 3.15 ( $\text{CH}_2(a)$ ), 3.27 ( $\text{CH}_2(d)$ ), 7.06 (2H meta pyridine), 7.62 (H para pyridine), 7.90 (H3), 8.00 (H8), 8.17 (H6), 8.21 (H5), 8.23 (2H ortho pyridine), 8.72 (H7), 9.49 (H2), 9.59 (H9);  $^{13}\text{C}$  NMR:  $\delta$  23.1, 26.2 ( $\text{CH}_2(b)$  and  $\text{CH}_2(c)$ ), 31.3 ( $\text{CH}_2(d)$ ), 52.9 ( $\text{CH}_2(a)$ ), 124.0 ( $\text{CH}(5)$ ), 126.1 ( $\text{CH}$

*meta* pyridine), 126.3 (CH(3)), 126.5 (CH(8)), 127.5 (CH(6)), 128.3 (CH(5)), 139.8 (CH(7)), 139.5 (CH *para* pyridine), 151.7 (CH *ortho* pyridine), 153.4 (CH(2)), 154.1 (CH(9)).

**Synthesis of the Ru-PhenISA Complex.** A sample of PhenISA (70 mg,  $9.4 \times 10^{-3}$  mmol of BAP) was dissolved in water (2.3 mL). The complex  $[\text{Ru}(\text{phen})_2(\text{CF}_3\text{SO}_3)_2]$  (7.1 mg,  $9.4 \times 10^{-3}$  mmol) then was added and the mixture heated via microwave irradiation (150 W, heating ramp: from 298 K to 323 K, 10 min; then, 323 K for 1 h). The solution color turned to orange. The sample was purified by ultracentrifugation (30 min at 7000 rpm at 293 K, filter cutoff = 3000 Da) two times. Finally, the polymeric complex was lyophilized to give a fluffy orange material. Elemental analysis: Found = C, 45.04; H, 7.23; N, 14.84; Ru, 1.39%, C/N, 3.04 (calcd for  $(\text{C}_{13}\text{H}_{22}\text{N}_4\text{O}_4)_{0.94}(\text{C}_{50}\text{H}_{43}\text{F}_6\text{N}_9\text{O}_{10}\text{S}_2\text{Ru})_{0.06}(\text{H}_2\text{O})_3$ , C, 44.91; H, 7.25; N, 14.80; Ru, 1.49%, C/N, 3.03). The  $^1\text{H}$  and  $^{13}\text{C}$  NMR signals of the PAA backbone were indistinguishable from those of PhenISA (reported in Table S1 in the Supporting Information). NMR data of the phenanthroline pendant ( $\text{H}_2\text{O}/\text{D}_2\text{O}$ , 9:1, pH 5.5; for the assignment of the BAP positions, see Chart S1 in the Supporting Information; the four signals of the protons of the two phen ligands on Ru are indicated by primed labels):  $^1\text{H}$  NMR  $\delta$  1.78 ( $\text{CH}_2(b)$  and  $\text{CH}_2(c)$ , m), 3.16 ( $\text{CH}_2(a)$ ), 3.25 ( $\text{CH}_2(d)$ ), 7.41 (1H, H3), 7.49 (1H, H8), 7.52 (4H, H3'), 7.91 (1H, H2), 7.92 (1H, H9), 7.95 (4H, H2'), 8.09 (4H, H5'), 8.18 (1H, H6), 8.34 (1H, H5), 8.47 (1H, H7), 8.54 (4H, H4');  $^{13}\text{C}$  NMR:  $\delta$  23.0, 26.5 ( $\text{CH}_2(b)$  and  $\text{CH}_2(c)$ ), 30.7 ( $\text{CH}_2(d)$ ), 52.8 ( $\text{CH}_2(a)$ ), 124.2 (1CH, C5), 124.6 (1CH, C9), 125.1 (1CH, C3), 125.3 (1CH, C8), 125.4 (4CH, C3'), 127.8 (1CH, C6), 127.9 (4CH, C5'), 130.0 ( $\text{C}_q$ , C4a), 130.4 ( $\text{C}_q$ , C7a), 130.7 (4 $\text{C}_q$ , C4a'), 136.5 (1CH, C7), 136.5 (4CH, C4'), 147.6 ( $\text{C}_q$ , C10a), 147.7 (4CH, C1a'), 149.7 ( $\text{C}_q$ , C1a), 151.7 (1CH, C2), 152.1 ( $\text{C}_q$ , C4), 152.2 (4CH, C2').

**Dynamic Light Scattering Measurements.** The average hydrodynamic diameters of the new PhenISA polymer and of its rhenium and ruthenium complexes were obtained by dynamic light scattering (DLS) measurements at 298 K. Samples were prepared by dispersing the freeze-dried polymers in filtered water (1 mg/mL Milli-Q water, 0.2  $\mu\text{m}$  syringe filter), setting the pH at the desired value via the addition of a few drops of 0.1 M NaOH or HCl directly into the cuvette. The refractive index and the viscosity of the solution were approximated to those of pure water at 298 K (1.33 and 0.8929 cP, respectively). The measurements were repeated at least three times, each repetition being the average of 10 scans of 60 s each.

**Stability of the Metal Complexes under Physiological Conditions in the Presence of Cysteine.** A sample of Re-PhenISA (4 mg) was dissolved in a 0.15 M NaCl solution (5 mL) at pH 7.2 (adjusted by the addition of a few drops of 0.1 M NaOH), affording a 0.14 mM solution (with respect to rhenium concentration), then cysteine (20 equiv) was added. The sample was introduced in a thermostated bath at 298 K and the stability was monitored through luminescence measurements at different times, using an aerated aqueous solution of  $[\text{Ru}(\text{bipy})_3]\text{Cl}_2$  as a standard. The stability assays of the Re-Py-PhenISA and Ru-PhenISA copolymers were performed in the same way.

**In Vitro Toxicity Assay.** HEK-293 cells were seeded in 96-well treated plates at a concentration of  $0.5 \times 10^6$  cells/mL in 100  $\mu\text{L}$  of Iscove Modified Dulbecco Medium (IMDM) supplemented with 10% heat-inactivated fetal bovine serum, 2 mM L-glutamine, penicillin–streptomycin, in the presence or absence of Re-Py-PhenISA and Ru-PhenISA at concentrations ranging from 0.5 to 50  $\mu\text{M}$ . After 24 h, the toxicity of the different complexes on HEK-293 cells was measured using the CellTiter–Blue Cell Viability Assay (Promega, Madison, WI, USA). In brief, 40  $\mu\text{L}$  of CellTiter-Blue were added in each well and, 3 h later, plates were read at 570 and 600 nm in a spectrofluorimeter and analyzed according to manufacturer instructions.

**Cell Uptake.** HEK-293 cells were incubated with ca. 5  $\mu\text{M}$  Ru-PhenISA for either 6 or 12 h before the start of the confocal imaging experiments:  $10^6$  cells per well were plated on tissue 6 wells plates in Dulbecco's modified Eagle's Medium (DMEM) supplemented with 10% heat-inactivated fetal bovine serum, 2 mM L-glutamine, penicillin–streptomycin (EuroClone), at 37  $^\circ\text{C}$  in a 5%  $\text{CO}_2$

atmosphere. The Ru-PhenISA fluorescence, collected between 420 and 650 nm, was excited by the 43  $\mu\text{W}$  output of the 458 nm line of the Ar<sup>+</sup> laser and both the emission and the transmitted light images were recorded at 400 Hz scan rate through a 40X HCX PL APO CS oil objective (N.A. = 1.3) after identification of the cellular focal plane by 1  $\mu\text{m}$  step z-scan measurements. Each image line is the average of five different measurements, with image dimensions being 512  $\times$  512 pixels, pixel size either 217 nm or 174 nm (image size = 111  $\mu\text{m}$   $\times$  111  $\mu\text{m}$  or 89  $\mu\text{m}$   $\times$  89  $\mu\text{m}$ , respectively). In order to discriminate between the emission of the complex and cellular autofluorescence, and to select the most appropriate wavelength acquisition range, spectral measurements were performed by recording the fluorescence images with a 5 nm step in the 475–650 nm range.

## ■ ASSOCIATED CONTENT

### Supporting Information

Supporting Information includes a table with the complete NMR data of PhenISA; a chart showing the numbering for NMR assignments; figures showing spectroscopic/photophysical details and cells toxicity assays. This material is available free of charge via the Internet at <http://pubs.acs.org>.

## ■ AUTHOR INFORMATION

### Corresponding Author

\*Tel.: +390250314352 (D.M.), +390250314132 (E.R.). Fax: +390250314405 (D.M.), 390250314129 (E.R.). E-mail: daniela.maggioni@unimi.it (D.M.), elisabetta.ranucci@unimi.it (E.R.).

### Present Address

<sup>1</sup>Institute of Inorganic Chemistry, University of Zurich, Winterthurerstrasse 190 CH-8057 Zurich, Switzerland.

### Notes

The authors declare no competing financial interest.

## ■ REFERENCES

- (1) (a) Patra, M.; Gasser, G. *ChemBioChem* **2012**, *13*, 1232–1252. (b) Haas, K. L.; Franz, K. J. *Chem. Rev.* **2009**, *109*, 4921–4960.
- (2) (a) Terreno, E.; Delli Castelli, D.; Viale, A.; Aime, S. *Chem. Rev.* **2010**, *110*, 3019–3042. (b) Kubiček, V.; Tóth, É. *Adv. Inorg. Chem.* **2009**, *61*, 63–129. (c) Aime, S.; Geninatti Crich, S.; Gianolio, E.; Giovenzana, G. B.; Teia, L.; Terreno, E. *Coord. Chem. Rev.* **2006**, *250*, 1562–1579. (d) Caravan, P.; Ellison, J. J.; McMurry, T. J.; Lauffer, R. B. *Chem. Rev.* **1999**, *99*, 2293–2352.
- (3) (a) Alberto, R. In *Medicinal Organometallic Chemistry*; Jaouen, G., Metzler-Nolte, N., Eds.; Topics in Organometallic Chemistry 32; Springer: Berlin, 2010; pp 219–246. (b) Liu, S. *Chem. Soc. Rev.* **2004**, *33*, 445–461.
- (4) See, for instance: (a) Lo, K. K.-W.; Choi, A. W.-T.; Law, W. H.-T. *Dalton Trans.* **2012**, *41*, 6021–6047. (b) Baggaley, E.; Weinstein, J. A.; Williams, J. A. G. *Coord. Chem. Rev.* **2012**, *256*, 1762–1785. (c) Zhao, Q.; Huang, C. H.; Li, F. Y. *Chem. Soc. Rev.* **2011**, *40*, 2508–2524. (d) Fernandez-Moreira, V.; Thorp-Greenwood, F. L.; Coogan, M. P. *Chem. Commun.* **2010**, *46*, 186–202. (e) Cosgrave, L.; Devocelle, M.; Forster, R. J.; Keyes, T. E. *Chem. Commun.* **2010**, *46*, 103–105. (f) Montgomery, C. P.; Murray, B. S.; New, E. J.; Pal, R.; Parker, D. *Acc. Chem. Res.* **2009**, *42*, 925–937. (g) Lau, J. S.-Y.; Lee, P.-K.; Tsang, K. H.-K.; Ng, C. H.-C.; Lam, Y.-W.; Cheng, S.-H.; Lo, K. K.-W. *Inorg. Chem.* **2009**, *48*, 708–718. (h) Koo, C.-K.; Wong, K.-L.; Man, C. W.-Y.; Lam, Y.-W.; So, L. K.-Y.; Tam, H.-L.; Tsao, S.-W.; Cheah, K.-W.; Lau, K.-C.; Yang, Y.-Y.; Chen, J.-C.; Lam, M. H.-W. *Inorg. Chem.* **2009**, *48*, 872–878. (i) Botchway, S. W.; Charnley, M.; Haycock, J. W.; Rochester, D. L.; Weinstein, J. A.; Williams, J. A. G. *Proc. Natl. Acad. Sci. U.S.A.* **2008**, *105*, 16071–16076.
- (5) Lakowicz, J. R.; Terpetschnig, E.; Murtaza, Z.; Szmajnski, H. J. *Fluoresc.* **1997**, *7*, 17–25.
- (6) See, for instance: (a) Thorp-Greenwood, F. L.; Coogan, M. P.; Mishra, L.; Kumari, N.; Rai, G.; Saripella, S. *New J. Chem.* **2012**, *36*,

- 64–72. (b) Lo, K. K. W.; Zhang, K. Y.; Li, S. P. Y. *Eur. J. Inorg. Chem.* **2011**, 24, 3551–3568. (c) Beck, D.; Brewer, J.; Lee, J.; McGraw, D.; DeGraff, B. A.; Demas, J. N. *Coord. Chem. Rev.* **2007**, 251, 546–553. (d) Blanco-Rodriguez, A. N.; Busby, M.; Grădinaru, C.; Crane, B. R.; Di Bilio, A. J.; Matousek, P.; Towrie, M.; Leigh, B. S.; Richards, J. H.; Vlček, A., Jr.; Gray, H. B. *J. Am. Chem. Soc.* **2006**, 128, 4365–4370. (e) Lo, K. K.-W.; Tsang, K. H.-K.; Sze, K.-S. *Inorg. Chem.* **2006**, 45, 1714–1722. (f) Guo, X.-Q.; Castellano, F. N.; Lakowicz, J. R. *Anal. Chem.* **1998**, 70, 632–637.
- (7) For same recent papers, see: (a) Mari, C.; Panigati, M.; D'Alfonso, L.; Zanoni, I.; Donghi, D.; Sironi, L.; Collini, M.; Maiorana, S.; Baldoli, C.; D'Alfonso, G.; Licandro, L. *Organometallics* **2012**, 31, 5918–5928. (b) Gasser, G.; Pinto, A.; Neumann, S.; Sosniak, A. M.; Seitz, M.; Merz, K.; Heumann, R.; Metzler-Nolte, N. *Dalton Trans.* **2012**, 41, 2304–2313. (c) Louie, M.-W.; Fong, T. T.-H.; Lo, K. K.-W. *Inorg. Chem.* **2011**, 50, 9465–9471. (d) Ferri, E.; Donghi, D.; Panigati, M.; Prencipe, G.; D'Alfonso, L.; Zanoni, I.; Baldoli, C.; Maiorana, S.; D'Alfonso, G.; Licandro, E. *Chem. Commun.* **2010**, 46, 6255–6257. (e) James, S.; Maresca, K. P.; Babich, J. W.; Valliant, J. F.; Doering, L.; Zubietta, J. *Bioconjugate Chem.* **2006**, 17, 590–596. (f) Lo, K. K.-W.; Tsang, K. H.-K.; Zhu, N. *Organometallics* **2006**, 25, 3220–3227. (g) Reece, S. J.; Seyedsayamdost, M. R.; Stubbe, J.; Nocera, D. G. *J. Am. Chem. Soc.* **2006**, 128, 13654–13655. (h) Lo, K. K.-W.; Hui, W.-K.; Chung, C.-K.; Tsang, K. H.-K.; Lee, T. K.-M.; Li, C.-K.; Lau, J. S.-Y.; Ng, D. C.-M. *Coord. Chem. Rev.* **2006**, 250, 1724–1736.
- (8) (a) Mauro, M.; Yang, C.-H.; Shin, C.-Y.; Panigati, M.; Chang, C.-H.; D'Alfonso, G.; De Cola, L. *Adv. Mater.* **2012**, 24, 2054–2058. (b) Li, X.; Zhang, D.; Chi, H.; Xiao, G.; Dong, Y.; Wu, S.; Su, Z.; Zhang, Z.; Lei, P.; Hu, Z.; Li, W. *Appl. Phys. Lett.* **2010**, 97, 263303–263306. (c) Mauro, M.; Quartapelle Procopio, E.; Sun, Y.; Chien, C.-H.; Donghi, D.; Panigati, M.; Mercandelli, P.; Mussini, P.; D'Alfonso, G.; De Cola, L. *Adv. Funct. Mater.* **2009**, 19, 2607–2614.
- (9) For the pioneer work in the field, see: Wrighton, M. S.; Morse, D. L. *J. Am. Chem. Soc.* **1974**, 96, 998–1003.
- (10) For some pertinent reviews, see: (a) Kumar, A.; Sun, S.-S.; Lees, A. J. *Top. Organomet. Chem.* **2010**, 29, 1–35. (b) Striplin, D. R.; Crosby, G. A. *Coord. Chem. Rev.* **2001**, 211, 163–175. (c) Stukfens, D. J., Jr.; Vlček, A. *Coord. Chem. Rev.* **1998**, 177, 127–179. (d) Lees, A. J. *Chem. Rev.* **1987**, 87, 711–743.
- (11) See, for instance: Villegas, J. M.; Stoyanov, S. R.; Huang, W.; Rillema, D. P. *Inorg. Chem.* **2005**, 44, 2297–2309.
- (12) Panigati, M.; Donghi, D.; Mauro, M.; Mercandelli, P.; Mussini, P.; De Cola, L.; D'Alfonso, G. *Coord. Chem. Rev.* **2012**, 256, 1621–1643.
- (13) Tseng, Y.-H.; Bhattacharya, D.; Lin, S.-H.; Thanasekaran, P.; Wu, J.-Y.; Lee, L.-W.; Sathiyendiran, M.; Ho, M.-L.; Chung, M.-W.; Hsu, K.-C.; Chou, P.-T.; Lu, K.-L. *Inorg. Chem.* **2010**, 49, 6805–6807.
- (14) (a) Quartapelle Procopio, E.; Mauro, M.; Panigati, M.; Donghi, D.; Mercandelli, P.; Sironi, A.; D'Alfonso, G.; De Cola, L. *J. Am. Chem. Soc.* **2010**, 132, 14397–14399. (b) Donghi, D.; D'Alfonso, G.; Mauro, M.; Panigati, M.; Mercandelli, P.; Sironi, A.; Mussini, P.; D'Alfonso, L. *Inorg. Chem.* **2008**, 47, 4243–4255.
- (15) (a) Fan, Y.; Li, C.; Cao, H.; Li, F.; Chen, D. *Biomaterials* **2012**, 33, 4220–4228. (b) Yang, T.; Xia, A.; Liu, Q.; Shi, M.; Wu, H.; Xiong, L.; Huang, C.; Li, F. *J. Mater. Chem.* **2011**, 21, 5360–5367. (c) Bryson, J.; Fichter, K. M.; Chu, W.-J.; Lee, J.-H.; Li, J.; Madsen, L. A.; McLendon, P.; Reineke, T. M. *Proc. Natl. Acad. Sci. U.S.A.* **2009**, 106, 16913–16918. (d) Liu, L.; Li, X.; Hou, S.; Xue, Y.; Yao, Y.; Ma, Y.; Feng, X.; He, S.; Lu, Y.; Wang, Y.; Zeng, X. *Chem. Commun.* **2009**, 44, 6759–6761. (e) Wu, Y.; Zhou, Y.; Ouari, O.; Woods, M.; Zhao, P.; Soesbe, T. S.; Kiefer, G. E.; Sherry, A. D. *J. Am. Chem. Soc.* **2008**, 130, 13854–13855.
- (16) (a) Larson, N.; Ghandehari, H. *Chem. Mater.* **2012**, 24, 840–853. (b) Hoffmann, S.; Vystrčilová, L.; Ulbrich, K.; Etrych, T.; Caysa, H.; Mueller, T.; Mäder, K. *Biomacromolecules* **2012**, 13, 652–663. (c) Khemtong, C.; Kessinger, C. W.; Gao, J. *Chem. Commun.* **2009**, 3497–3510. (d) Saad, M.; Garbuzenko, O. B.; Ber, E.; Chandna, P.; Khandare, J. J.; Pozharov, V. P.; Minko, T. *J. Controlled Release* **2008**, 130, 107–114. (e) Kim, J. H.; Park, K.; Nam, H. Y.; Lee, S.; Kim, K.; Kwon, I. C. *Prog. Polym. Sci.* **2007**, 32, 1031–1053.
- (17) Fox, M. E.; Szoka, F. C.; Fréchet, J. M. J. *Acc. Chem. Res.* **2009**, 42, 1141–1151.
- (18) (a) Louie, A. *Chem. Rev.* **2010**, 110, 3146–3195. (b) Jennings, L. E.; Long, N. J. *Chem. Commun.* **2009**, 24, 3511–3524.
- (19) Ferruti, P.; Marchisio, M. A.; Duncan, R. *Macromol. Rapid Commun.* **2002**, 23, 332–355.
- (20) Ranucci, E.; Ferruti, P.; Lattanzio, E.; Manfredi, A.; Rossi, M.; Mussini, P. R.; Chiellini, F.; Bartoli, C. *J. Polym. Sci., Part A: Polym. Chem.* **2009**, 47, 6977–6991.
- (21) (a) Cavalli, R.; Bisazza, A.; Sessa, R.; Primo, L.; Fenili, F.; Manfredi, A.; Ranucci, E.; Ferruti, P. *Biomacromolecules* **2010**, 11, 2667–2674. (b) Ferruti, P.; Franchini, J.; Bencini, M.; Ranucci, E.; Zara, G. P.; Serpe, L.; Primo, L.; Cavalli, R. *Biomacromolecules* **2007**, 8, 1498–1504.
- (22) Richardson, S. C. W.; Patrick, N. G.; Lavignac, N.; Ferruti, P.; Duncan, R. *J. Controlled Release* **2010**, 142, 78–88.
- (23) Richardson, S.; Ferruti, P.; Duncan, R. *J. Drug Targeting* **1999**, 6, 391–404.
- (24) Donghi, D.; Maggioni, D.; D'Alfonso, G.; Amigoni, F.; Ranucci, E.; Ferruti, P.; Manfredi, A.; Fenili, F.; Bisazza, A.; Cavalli, R. *Biomacromolecules* **2009**, 10, 3273–3282.
- (25) Mindt, T.; Struthers, H.; Garcia-Garayoa, E.; Desbouis, D.; Schibli, R. *Chimia* **2007**, 61, 725–731.
- (26) Ruggi, A.; Beekman, C.; Wasserberg, D.; Subramaniam, V.; Reinhoudt, D. N.; van Leeuwen, F. W. B.; Velders, A. H. *Chem.—Eur. J.* **2011**, 17, 464–467.
- (27) See, for instance: (a) Ho, C.-L.; Wong, W.-Y. *Coord. Chem. Rev.* **2011**, 255, 2469–2502. (b) Marin, V.; Holder, E.; Hoogenboom, R.; Schubert, U. S. *Chem. Soc. Rev.* **2007**, 36, 618–635. (c) Chan, W. K. *Coord. Chem. Rev.* **2007**, 251, 2104–2118. (d) Carlise, J. R.; Weck, M. *J. Polym. Sci. A: Polym. Chem.* **2004**, 42, 2973–2984. (e) Zhang, M.; Lu, P.; Wang, X.; He, L.; Xia, H.; Zhang, W.; Yang, B.; Liu, L.; Yang, L.; Yang, M.; Ma, Y.; Feng, J.; Wang, D.; Tamai, N. *J. Phys. Chem. B* **2004**, 108, 13185–13190.
- (28) Several somewhat related systems have to be mentioned. Besides the polyamidoamine dendrimers decorated with Ru polypyridyl complexes, quoted above,<sup>26</sup> we mention the block copolymers containing Ru(phen)<sub>3</sub><sup>2+</sup> groups, able to give micellar assemblies in mixed organic-aqueous media,<sup>29</sup> as well as the lactic acid-PEG co-oligomers binding Re(CO)<sub>3</sub> fragments,<sup>30</sup> or the dendritic oligomers bearing cyclometalated iridium(III) bipyridine complexes.<sup>31</sup>
- (29) Sankaran, N. B.; Rys, A. Z.; Nassif, R.; Nayak, M. K.; Metera, K.; Chen, B.; Bazzi, H. S.; Sleiman, H. F. *Macromolecules* **2010**, 43, 5530–5537.
- (30) Zhu, H.; Xu, X. P.; Cui, W.; Zhang, Y. Q.; Mo, H. P.; Shen, Y. M. *J. Polym. Sci., Part A: Polym. Chem.* **2009**, 49, 1745–1752.
- (31) Zhang, K. Y.; Liu, H.-W.; Fong, T. T.-H.; Chen, X.-G.; Lo, K. K.-W. *Inorg. Chem.* **2010**, 49, 5432–5443.
- (32) Amoroso, A. J.; Coogan, M. P.; Dunne, J. E.; Fernandez-Moreira, V.; Hess, J. B.; Hayes, A. J.; Lloyd, D.; Millet, C.; Pope, S. J. A.; Williams, C. *Chem. Commun.* **2007**, 3066–3068.
- (33) Wang, Z.; McWilliams, A. R.; Evans, C. E. B.; Lu, X.; Chung, S.; Winnik, M. A.; Manners, I. *Adv. Funct. Mater.* **2002**, 12, 415–419.
- (34) See, for instance: (a) Crosby, G. A.; Perkins, W. G.; Klassen, D. M. *J. Chem. Phys.* **1965**, 43, 1498–1503. (b) Nakamaru, K. *Bull. Chem. Soc. Jpn.* **1982**, 55, 2697–2705.
- (35) Bandyopadhyay, B. N.; Harriman, A. *J. Chem. Soc., Faraday Trans. 1* **1977**, 73, 663–674.
- (36) Salignac, B.; Grundler, P. V.; Cayemittes, S.; Frey, U.; Scopelliti, R.; Merbach, A. E.; Hedinger, R.; Hegetschweiler, K.; Alberto, R.; Prinz, U.; Raabe, G.; Kollle, U.; Hall, S. *Inorg. Chem.* **2003**, 42, 3516–3526.
- (37) Alberto, R.; Schibli, R.; Waibel, R.; Abram, U.; Schubiger, A. P. *Coord. Chem. Rev.* **1999**, 190–192, 901–919.
- (38) Probst, B.; Guttentag, M.; Rodenberg, A.; Hamm, P.; Alberto, R. *Inorg. Chem.* **2011**, 50, 3404–3412.

(39) Frederiks, S. M.; Luong, J. M.; Wrighton, M. S. *J. Am. Chem. Soc.* **1979**, *101*, 7415–7418.

(40) The IR spectrum bears resemblance to that of  $[\text{Re}(\text{CO})_3\text{Cl}(\text{phen})]$  (2024(s), 1920(m), 1898(m)  $\text{cm}^{-1}$ , in acetonitrile),<sup>39</sup> but the formation of this species can be ruled out, because the presence of chloride anions was carefully avoided in all the steps of the synthesis of PhenISA. To support the hypothesis of carboxylate coordination, the complex  $[\text{Re}(\text{CO})_3(\text{O}_2\text{CCH}_3)(\text{BAP})]$  has been prepared (see the Experimental Section) and shown to display very similar CO stretching bands (2025(s) and 1919(vs)  $\text{cm}^{-1}$  in ethanol, see Figure S7 in the Supporting Information).

(41) It is also worth adding that the short component of the lifetime cannot be attributed to the hypothetical chloro-derivative  $[\text{Re}(\text{CO})_3\text{Cl}(\text{phen})]$ , whose presence might be inferred from the IR spectrum (see ref 40), because a lifetime of 300 ns was measured for such species (even if in deaerated dichloromethane).<sup>9</sup>

(42) Moore, S. A.; Frazier, S. M.; Sibbald, M. S.; DeGraff, B. A.; Demas, J. N. *Langmuir* **2011**, *27*, 9657–9675.

(43) Friedman, A. E.; Chambron, J.-C.; Sauvage, J.-P.; Turro, N. J.; Barton, J. K. *J. Am. Chem. Soc.* **1990**, *112*, 4960–4962.

(44) Wolcan, E.; Torchia, G.; Tocho, J.; Piro, O. E.; Juliarena, P.; Ruiz, G.; Féliz, M. R. *J. Chem. Soc., Dalton Trans.* **2002**, 2194–2202.

(45) For a recent comprehensive review, see: Campagna, S.; Puntoriero, F.; Nastasi, F.; Bergamini, G.; Balzani, V. *Top. Curr. Chem.* **2007**, *280*, 117–214.

(46) Grätzel, M. *Acc. Chem. Res.* **2009**, *42*, 1788–1798.

(47) For some recent references, see: (a) Svensson, F. R.; Andersson, J.; Åmand, H. L.; Lincoln, P. *J. Biol. Inorg. Chem.* **2012**, *17*, 565–571. (b) Matson, M.; Svensson, F. R.; Nordén, B.; Lincoln, P. *J. Phys. Chem. B* **2011**, *115*, 1706–1711. (c) Pisani, M. J.; Fromm, P. D.; Mulyana, Y.; Clarke, R. J.; Korner, H.; Heimann, K.; Collins, J. G.; Keene, F. R. *ChemMedChem* **2011**, *6*, 848–858.

(48) (a) Zhang, R.; Ye, Z.; Yin, Y.; Wang, G.; Jin, D.; Yuan, J.; Piper, J. A. *Bioconjugate Chem.* **2012**, *23*, 725–733. (b) Zhang, R.; Ye, Z.; Wang, G.; Zhang, W.; Yuan, J. *Chem.—Eur. J.* **2010**, *16*, 6884–6891. (c) O'Connor, N. A.; Stevens, N.; Samaroo, D.; Solomon, M. R.; Marti, A. A.; Dyer, J.; Vishwasrao, H.; Akins, D. L.; Kandel, E. R.; Turro, N. J. *Chem. Commun.* **2009**, 2640–2642.

(49) (a) Gill, M. R.; Thomas, J. A. *Chem. Soc. Rev.* **2012**, *41*, 3179–3192. (b) Keene, F. R.; Smith, J. A.; Collins, J. G. *Coord. Chem. Rev.* **2009**, *253*, 2021–2035. (c) Zeglis, B. M.; Pierre, V. C.; Barton, J. K. *Chem. Commun.* **2007**, 4565–4579.

(50) Tian, X.; Gill, M. R.; Cantón, I.; Thomas, J. A.; Battaglia, G. *ChemBioChem* **2011**, *12*, 548–551.

(51) Pazderski, L.; Pawlak, T.; Sitkowski, J.; Kozerski, L.; Szlyk, E. *Magn. Reson. Chem.* **2010**, *48*, 450–457.

(52) Juris, A.; Balzani, V.; Barigiletti, F.; Campagna, S.; Belser, P.; Von Zelewsky, A. *Coord. Chem. Rev.* **1988**, *84*, 85–277.

(53) Griffiths, P. C.; Paul, A.; Khayat, Z.; Wan, K.-W.; King, S. M.; Grillo, I.; Schweins, R.; Ferruti, P.; Franchini, J.; Duncan, R. *Biomacromolecules* **2004**, *5*, 1422–1427.

(54) Massignani, M.; LoPresti, C.; Blanazs, A.; Madsen, J.; Armes, S. P.; Lewis, A. L.; Battaglia, G. *Small* **2009**, *21*, 2424–2432.

(55) (a) Causey, P. W.; Besanger, T. R.; Schaffer, P.; Vaillant, J. F. *Inorg. Chem.* **2008**, *47*, 8213–8221. (b) Schibli, R.; Schwarzbach, R.; Alberto, R.; Ortner, K.; Schmale, H.; Dumas, C.; Egli, A.; Schubiger, A. *Bioconjugate Chem.* **2002**, *13*, 750–756.

(56) Pascu, S. I.; Waghorn, P. A.; Conry, T.; Lin, B.; James, C.; Zayed, J. M. *Adv. Inorg. Chem.* **2009**, *61*, 131–178.

(57) (a) Schaffer, P.; Gleave, J. A.; Lemon, J. A.; Reid, L. C.; Pacey, L. K. K.; Farncombe, T. H.; Boreham, D. R.; Zubieta, J.; Babich, J. W.; Doering, L. C.; Valliant, J. F. *Nucl. Med. Biol.* **2008**, *35*, 159–169. (b) Stephenson, K. A.; Banerjee, S. R.; Besanger, T.; Sogbein, O. O.; Levadala, M. K.; McFarlane, N.; Lemon, J. A.; Boreham, D. R.; Maresca, K. M.; Brenna, J. D.; Babich, J. W.; Zubieta, J.; Valliant, J. J. *J. Am. Chem. Soc.* **2004**, *126*, 8598–8599.

(58) (a) Azad, B. B.; Cho, C. F.; Lewis, J. D.; Luyt, L. G. *Appl. Radiat. Isot.* **2012**, *70*, 505–511. (b) Thorp-Greenwood, F. L.; Coogan, M. P. *Dalton Trans.* **2011**, *40*, 6129–6143. (c) Boulay, A.; Artigau, M.;

Coulais, Y.; Picard, C.; Mestre-Voegtle, B.; Benoist, E. *Dalton Trans.* **2011**, *40*, 6206–6209. (d) Agorastos, N.; Borsig, L.; Renard, A.; Antoni, P.; Viola, G.; Spingler, B.; Kurz, P.; Alberto, R. *Chem.—Eur. J.* **2007**, *13*, 3842–3852.

(59) Ferruti, P.; Ranucci, E.; Trotta, F.; Gianasi, E.; Evagorou, G. E.; Wasil, M.; Wilson, G.; Duncan, R. *Macromol. Chem. Phys.* **1999**, *200*, 1644–1654.

(60) Schmidt, S.; Trogler, W.; Basolo, F. *Inorg. Synth.* **1985**, *23*, 41–46.

(61) Schmidt, S.; Nitschke, J.; Trogler, W. *Inorg. Synth.* **1989**, *26*, 113–117.

(62) He, H.; Lipowska, M.; Xu, X.; Taylor, A. T.; Carlone, M.; Marzilli, L. *Inorg. Chem.* **2005**, *44*, 5437–5446 (slightly modified by the addition of a small amount of  $\text{CF}_3\text{SO}_3\text{H}$  before refluxing, see ref 24).

(63) Sullivan, B. P.; Salmon, D. J.; Meyer, T. J. *Inorg. Chem.* **1978**, *17*, 3334–3341.

(64) Greaney, M. A.; Coyle, C. L.; Harmer, M. A.; Jordan, A.; Stiefel, E. I. *Inorg. Chem.* **1989**, *28*, 912–920.

(65) Grythe, K. F.; Hansen, F. K.; Walderhaug, H. *J. Phys. Chem. B* **2004**, *108*, 12404–12412.

(66) Stilbs, P. *Prog. Nucl. Magn. Reson. Spectrosc.* **1987**, *19*, 1–45.

(67) Ishida, A.; Tobita, S.; Hasegawa, Y.; Katoh, R.; Nozaki, K. *Coord. Chem. Rev.* **2010**, *254*, 2449–2458.

(68) Lakowicz, J. R. *Principles of Fluorescence Spectroscopy*, 2nd ed.; Kluwer Academic/Plenum Publishers: New York, 1999.

(69) Collini, M.; Chirico, G.; Baldini, G.; Bianchi, M. E. *Biopolymers* **1995**, *36*, 211–225.

(70) Freddi, S.; D'Alfonso, L.; Collini, M.; Caccia, M.; Sironi, L.; Tallarida, G.; Caprioli, S.; Chirico, G. *J. Phys. Chem. C* **2009**, *113*, 2722–2730.

(71) Macchioni, A.; Ciancaleoni, G.; Zuccaccia, C.; Zuccaccia, D. *Chem. Soc. Rev.* **2008**, *37*, 479–489.